

**MONITORING THE EFFECTS OF DROUGHT ON CROP YIELD IN THE LOWER
MEKONG BASIN**

By

Abhijeet Abhishek

A THESIS

Submitted to
Michigan State University
in partial fulfillment of the requirements
for the degree of

Civil Engineering – Master of Science

2018

ABSTRACT

MONITORING THE EFFECTS OF DROUGHT ON CROP YIELD IN THE LOWER MEKONG BASIN

By

Abhijeet Abhishek

Recurring drought in the Lower Mekong region has resulted in the need of a monitoring system for assessing the subtle, intrinsic nature of drought. Therefore, the objective of this study is to test an integrated modeling system that simulates the hydrological variables, drought characteristic, and crop yield over the Lower Mekong Basin. This study uses a coupled hydrologic and crop modeling framework- Regional Hydrologic Extremes Assessment System (RHEAS) over Cambodia in Lower Mekong Basin, which provides different drought severity measures and end-of-season crop yield estimates for 2000-2016. Gridded meteorological data were forced to the hydrologic model at a spatial resolution of 0.25° to estimate the fundamental drought characteristics, whereas the outputs from the hydrologic model were further used as forcing for the crop model. The validation of the RHEAS outputs was done using more than 3 years of soil moisture data from the SMAP mission. A good correlation ($r=0.8$) was obtained between the simulated RHEAS-based surface soil moisture data and the SMAP data over Cambodia, providing confidence to the model performance. For the crop model performance, yield estimates were compared against the observed rice yields from FAO. The simulated yield and observed yield also exhibited a good correlation ($R^2=0.83$) for years 2008-2016, while the initial simulation years (2000-2008) showed a substantial bias between observed and model estimates. We envisage that RHEAS will improve the management of drought-related risks on agriculture in the Lower Mekong Basin countries for better decision making.

ACKNOWLEDGEMENTS

At the onset, I would like to thank my advisor Dr. Mantha S. Phanikumar for accepting me as a Master student at Michigan State for which I'll indebted to him. I would like to my express my deepest gratitude to my co-advisor Dr. Amor V.M Ines, with whom I got a chance to work for two valuable years. His inspiring and invaluable guidance, encouragement and patience with me is something I would cherish forever. This thesis would not have been completed without his efforts and guidance.

Special mention to Dr. Narendra N. Das for helping me in the thesis, who was actively engaged in the works of this research. Without his input and passionate participation, the research could not have been successfully conducted.

I would like to thank my committee members, Dr. Yadu Pokhrel and Dr. Jeffrey Andresen for serving on my thesis committee and providing appropriate suggestion and comments to improve this thesis.

I would like to mention special thanks to my lab members Eeswaran Rasu and Prakash Jha for accompanying and helping me at the time of need by giving valuable advice and suggestion regarding the research and other things.

Finally, I would like to my thank my parents for providing me with continuous support and encouragement throughout my years of study.

TABLE OF CONTENTS

LIST OF TABLES	vi
LIST OF FIGURES	vii
Chapter 1	1
INTRODUCTION	1
1.1. Introduction	1
1.2. Research Objectives	4
1.3. Significance of the Research	4
1.4. Organization of Thesis	5
Chapter 2	7
LITERATURE REVIEW	7
2.1. Introduction	7
2.2. Drought: The Concept	9
2.3. Overview of the Cropping Sector	13
2.4. RHEAS: Software Description	16
Chapter 3	21
SITE DESCRIPTION	21
3.1. Location and Description	21
3.1.1. Topography and land-Use	21
3.1.2. Geology	24
3.1.3. Hydroclimate	24
3.1.4. Biodiversity	24
3.1.5. Socioeconomic conditions	24
3.1.6. Navigation	25
Chapter 4	26
DATA AND METHODS	26
4.1. Setting up the model	26
4.2. Data Acquisition	26
4.3. Methodology	29
4.3.1. Hydrologic Modeling	29
4.3.2. Crop Modeling	33
4.3.3. Nowcast Simulations	36
Chapter 5	40
RESULTS AND DISCUSSIONS	40
5.1. Technical Validation	40
5.1.1. Hydrologic Model Validation	40
5.1.2. Crop Model Validation	42
5.2. Hydrologic Modeling: VIC	44

5.3. Crop Modeling: DSSAT	48
5.4. Technical Analyses: Impact of Drought on Rice Yields	51
Chapter 6	54
CONCLUSION	54
BIBLIOGRAPHY	56

LIST OF TABLES

Table 1. Country wise projected yield of rice in 2025 and 2050 over Lower Mekong region (source: MRC, 2014)	15
Table 2. Available datasets in the RHEAS database along with spatial and temporal resolution .	19
Table 3. Meteorological conditions based on classification of standardized precipitation index (SPI) (source: McKee et al., 1993)	32
Table 4. Meteorological conditions based on classification of Soil Moisture Deficit Index (SMDI) (source: Narasimhan and Srinivasan., 2005).....	33
Table 5. Genotype coefficients for two rice cultivars for Cambodia, used in the crop model	39

LIST OF FIGURES

Figure 1. Actual (1990-2012) and projected rice yield in LMB for 2025 and 2050 under climate change. (source: MRC, 2014)	15
Figure 2. Schematic view of the Regional Hydrological Extremes Assessment Systems (RHEAS) framework	16
Figure 3. Schematic view of the RHEAS algorithm with remotely sensed datasets to provide hydro-climatic states and indicators.....	17
Figure 4. Map of the Mekong River Basin (top); Location of the four countries in Lower Mekong Basin (bottom left); Elevation map of the study area: Cambodia (bottom right)	22
Figure 5. Land-use pattern over Cambodia.....	23
Figure 6. A typical Data Configuration File, providing the dimensions of the study area, along with the source and duration of the ingested datasets.....	27
Figure 7. Precipitation values for each day in the 'prec' table of 'lmb' schema stored as raster in RHEAS database.....	28
Figure 8. Schematic representation of the variable infiltration capacity (VIC) hydrological model (http://www.hydro.washington.edu/Lettenmaier/Models/VIC)	30
Figure 9. Fertilizer Consumption (kilograms per hectare of arable land) of Cambodia from 2000-2017.....	35
Figure 10. Sample Yield Table stored in a schema within the RHEAS database	36
Figure 11. Nowcast Configuration File, showing the hydrologic simulation for Cambodia.....	37
Figure 12. Comparison between RHEAS based surface soil moisture for 2017 data when compared with the SMAP surface soil moisture data (L3_SM_P) at 36 km EASE2 grid resolution.....	41
Figure 13. Unbiased RMSE: RHEAS based surface soil moisture for 2016 and 2017 data when compared with the SMAP surface soil moisture data (L3_SM_P) at 36 km EASE2 grid resolution (left); Correlation: RHEAS based surface soil moisture for 2016 and 2017 data when compared with the SMAP surface soil moisture data (L3_SM_P) at 36 km EASE2 grid resolution (right)	41
Figure 14. Comparison of actual yield records from FAO and RHEAS (DSSAT) simulations for rice in Cambodia from 2000-2016.....	43

Figure 15. Best fit result between observed and model simulated rice yields from 2008-2016....	43
Figure 16. 3-month Standardized Precipitation Index over Cambodia for Feb-Mar-Apr (left), and Jun-Jul-Aug (right)	45
Figure 17. Agricultural drought severity over Cambodia for Mar-Apr-May (left), and Jun-Jul-Aug (right)	45
Figure 18. Spatial Distribution of Soil Moisture Deficit Index (SMDI) over Cambodia in 22nd week (last week of May) of 2015 (left), and 33rd week of 2015 (third week of August) (right) .	46
Figure 19. Annual Precipitation over Cambodia in 2015 for Mar-Apr-May (left), and Jul-Aug-Sep (right)	47
Figure 20. Dryspells period over Cambodia for Mar-Apr-May (left), and Aug-Sep-Oct (right) .	47
Figure 21. Annual precipitation (mm/year) time series over Cambodia from 2000-2016	48
Figure 22. RHEAS (DSSAT) Output: Map of rice yield over Cambodia in 2005 (left) and 2015 (right) disaggregated to province level	49
Figure 23. Rice Yields for each province of Cambodia from 2000-2016	49
Figure 24. Provincial Rice yields over Cambodia from 2000-2016	50
Figure 25. Correlation between 3-month SPI and rice yield over all provinces of Cambodia for J-J-A, 2000-2016	52
Figure 26. Correlation between 3-month SPI and rice yield for J-J-A from 2000-16 over Kampot (top), and Kandal (bottom) province of Cambodia.....	53

Chapter 1.

INTRODUCTION

1.1. Introduction

Developing countries, especially, in Asia and Africa face tremendous challenges pertaining to food security due to population growth, rapid urbanization, shrinking croplands, weather extremes and climate change (Godfray et al., 2010). Asia holds 60 percent of the global population and expected to increase to 64 percent in 2050 (United Nations, 2014). The glimpse of climate change is also distinctly evident in Asia that includes the Lower Mekong Basin (LMB) countries (Thailand, Lao PDR, Cambodia, and Viet Nam). These countries are prone to extreme events like floods, droughts, and tropical storms in recent years, and the trends have increased the vulnerability of the region to the negative consequences of climate change. Thus, posing a risk for humans, the agricultural setup and the natural ecosystem. LMB countries have also been heavily impacted by the recent weather- and climate-related changes attributed to global warming (IPCC., 2014). This strongly implies that LMB countries in future will experience more frequent occurrence and prolonged duration of droughts (Wang et al., 2016; Sheffield et al., 2012).

The Mekong river passing through the LMB countries is an important trans-boundary river, with an estimated length of 4,909 km. The basin has a mean estimated annual volume of 475 cu.km and 810,000 sq.km drainage, making it the 12th-longest river in the world (MRC 2010; MRC 2015; Liu et al., 2009). The Mekong river originates from the Tibetan plateau, flows 2500 km through China, 2400 km through Laos and Myanmar, Thailand, Cambodia, and Vietnam before it drains into the South China Sea. About 77 percent of the river flowing through the lower portion of the basin and coverage area of 606,000 sq. km consisting of the four riparian LMB countries, the area is recognized as imperative, both environmentally and economically. The impacts of climate

change have been prominent in the southern stretches of the Mekong Basin. High temperatures, dry periods, along with the El Nino events account for the majority of the disturbances in the regional climate (Thirumalai et al., 2017). Climate change alters the hydrologic cycle, resulting in seasonal water shortages. On the other hand, these changes, combined with increased temperatures, increases the risk of drought in the region. Since last two decades, extreme drought events occurred during 1997-98 and 2003-05 (IPCC., 2007), the worst of them being in late 2015 until July 2016, having widespread impacts over the four riparian countries (Son et al., 2012; Guo et al., 2017). Impacts from drought have had major issues on agriculture, forestry, water resources, and the environment in the LMB, where severe droughts in 2015 and 2016 had a major impact on the availability of water and agricultural productivity in the region. The droughts have a major impact on the food demand of the growing population, with more than 70 percent of the population dependent on agriculture for their livelihood (FAO/MoP 2010; MRC 2003; MRC 2009). Chhinh et al. (2015) reported damage of 200-1000 hectares of paddy rice in a Cambodian province, from 1994 and 2006. The prevalence of climate-related hazards, such as droughts and floods, have an enormous impact on the social and economic conditions of the farmers. The people in the region are poor and stay in rural settings, making them vulnerable to the risks and uncertainties associated with seasonality. With no other alternative source of income other than agriculture, the situation is a disaster for the families of farmers. As the majority of agricultural production in the region are rain-fed, there are huge crop losses from drought events (MAFF, 2010; SWC 2006). These events are sometimes associated with the changes in the global atmospheric circulation, which brings about a variable climate. The severe flooding events and low crop yields in the Mekong Basin are associated with warm ENSO events, which causes strong anomalies in winds and sea surface temperature.

Rice being the major crop in the region is sensitive to climate, and the most likely to be affected by extreme events (e.g. floods and droughts) (Chhinh et al., 2015; Christensen et al., 2007; MRC., 2015). The estimated dependence on rice is expected to increase from 2.7 billion to 3.9 billion by 2025 (International Rice Research Institute, 2007). To meet this huge demand in future, better management practices and advanced technologies are necessary for local as well as regional scale. Despite various advancements in agricultural and management practices, there has been a constant gap between science organizations and end-users, resulting in the partial implementation of effective adaption strategies (Andreadis et al., 2017). This fundamental disconnect between scientists and end-users is very much noticed within the agriculture sector, so bridging the gap will help policymakers facilitate better decision making. Understanding the impacts of drought on agricultural productivity can improve the standard of living for the people in the Lower Mekong Basin. Thus, the need of better techniques for monitoring and managing the climatic variabilities, and its impact on water stress and food production is essential for improving the decision-making and operational capabilities of the local policy-makers for drought management (Hao et al., 2017). Monitoring drought will also result in the effective management of water resources, resulting in minimal losses in agricultural productivity. With the recent development of numerous remote sensing approaches, mapping and monitoring drought, vegetation growth, soil conditions (moisture), temperature have proved to be helpful for giving an accurate estimation of crop conditions and water management practices. The integration of multiple remote sensing products across every component of the hydrologic cycle into a comprehensive drought monitoring system can be helpful in providing information about the onset, severity, spatial extent of drought. A remote-sensing constrained hydrologic modeling framework, Regional Hydrologic Extremes Assessment System (RHEAS), was implemented at the NASA/SERVIR project in Lower Mekong

Basin for monitoring drought and evaluating its impact on agricultural productivity in the region. The study aims to have a better understanding of the regional and environmental conditions related to hydrology and crop yield to facilitate improved decision-making processes.

1.2. Research Objectives

The overall goal of this study is to simulate the rice crop yield and determine the influence of drought on crop yield in the recent past in one of the Lower Mekong Basin country (Cambodia).

Two specific objectives are required to achieve the overall goal, they are:

- I. Studying the meteorological and agriculture droughts in Cambodia to assess drought evolution over a period of last two decades.
- II. Estimating the rice crop yield in Cambodia and evaluating the impact of various drought indicators on the crop growth/development and the rice yield.

1.3. Significance of the Research

LMB is facing the worst consequences of climate change, as a result of recent physiographic and demographic shifts. The LMB countries are increasingly becoming prone to the effects of extreme events, such as flood and drought. The damages from these events impose immense pressure on the region's economy, leading to various socio-economic challenges such as an increase in food prices, food security, and famine. Droughts significantly affect the agricultural productivity, affecting the vast rural population of LMB, who are substantially dependent on agriculture for their livelihood. As the demand for agricultural products set to increase in the future, the climate-related changes are constraining the rate of present development. The production of rice, in particular, is experiencing the maximum impact from droughts and floods, due to limited irrigation and dry season drought. Despite previous studies on drought monitoring, there has been less stress towards vulnerability of agriculture to drought because of its gradual and subtle development over

time. The use of earth observation systems, in-situ data, and statistical modeling techniques have gained popularity in recent times. Numerous studies have been carried out to effectively monitor drought and its various impacts on agriculture, water scarcity. Many drought monitoring techniques have been used in the past, from traditional methods (in-situ observations) to the present use of different remote-sensing based indices, which is elaborated in Chapter 2. The RHEAS framework has already been used successfully for monitoring drought and crop yield (maize) over large regions in East Africa (Das et al, submitted). This study aims to test the ability of RHEAS framework to effectively monitor drought variables, and its impact on rice yield in Lower Mekong Basin to support policymakers in facilitating improved decision-making during the growing season.

1.4. Organization of Thesis

The thesis consists of six chapters in total. The "Introduction" briefly discusses the rapid urbanization matched with population growth creating immense pressure on natural resources, and the ecosystem, which results in variability of regional climate leading to extreme events. The main goal and specific objectives of the research were also outlined, followed by the significance of the proposed study. The Chapter 2-"Literature Review" discusses the theoretical and methodological aspects of the research topic in details. The various aspects of drought monitoring, both traditional and advanced, advantages of new techniques, agricultural practices in the study area, and new findings in the research has been discussed in detail. The proposed research framework has also been presented in the section, including the design and constituent components. The Chapter 3-"Site Description" outlines the different characteristics, such as topography, hydro-climate, of the study region. Chapter 4-"Data and Methods" presents the list of datasets used for model simulations, along with their sources and working characteristics, and methodology presenting the

approach of the work from model setup until calibration and validation. Chapter 5-"Results and Discussion" section discusses the results of the simulations with Chapter 6-"Conclusion" summarizing the conceptual findings of the work, along with recommendations for future studies.

Chapter 2.

LITERATURE REVIEW

2.1. Introduction

According to the recent reports by the United Nations, the global population in 2018 stands at 7.7 billion, expected to increase to 9.8 billion in 2050 (source: World Population Prospects: The 2017 Revision). Asia will continue to be the most populous continent, with 60 percent of the world's population (source: World Population Prospects, 2017 Revision; United Nations, 2015a). Lately, Asia has been experiencing observable effects of anthropogenic climate change, with rising trends of global warming, increased intensity and/or frequency of extreme events (Climate Change 2014 Report, IPCC). Human-related activities remain the dominant reason for the unprecedented warming over the last decade. The exuberance and careless use of natural resources are imposing a serious threat on the planet. The increased emissions of greenhouse gases, deforestation, burning of fossil fuels (oil, gas or coal), and farming livestock are some of the major factors contributing to the change in climatic conditions. The burning of fossil fuels accounts for the majority of energy usage in day-to-day lives. The discovery of alternative types of energy like wind and solar power didn't replace the existing fuels, instead fueled additional growth. About 81 percent of the global energy demand is obtained from fossil fuels, while only 20 percent of global primary energy supply is contributed from renewable sources (source: Renewable Global Status Report, 2017; Global Energy and CO2 status Report, IEA, 2017). Crude oil remains the largest energy source globally, followed by coal and natural gas, with maximum growth in Asia, particularly China and India. Southeast Asia and Africa also showed an upward trend in their energy consumption, with Southeast Asia's energy demand growing by 60 percent in the last two decades (source: Southeast Asia Energy Outlook, IEA, 2017). The burning of fossil fuels results in the production of most

greenhouse gases, that traps the heat of the sun that is unable to escape, thereby warming the surface of the earth and lower atmosphere. Other factors like extensive deforestation for human settlements and the substantial amount of agricultural emissions also adds an enormous amount of greenhouse gases, resulting in warmer conditions. The warmer conditions tend to increase overall evaporation and precipitation, leading to the melting of glaciers contributing to sea level rise. As the Earth's temperature continues to rise, there is a significant impact on the earth's freshwater resources. Glaciers are one of the important sources of freshwater, which are disappearing at an unprecedented rate. There have been several shreds of evidence of changes in glaciers and ice caps, leading to increased river runoff and discharge peaks (Box et al., 2006, Jansson et al., 2003). NASA's Gravity Recovery and Climate Experiment showed about 281 billion tons decrease of ice sheets in Antarctica and Greenland. The climate components, temperature, and precipitation play a major role in influencing the earth's climate. An increase of 0.9 °C has been occurring since the late 19th century, with 2016 being recorded as the warmest year. The impacts of climate variability are sensed all around the world, with more relevance impacts in Asia. The huge population of Asia is extensively impacted by enormous environmental stresses, such as urbanization, global warming, water scarcity, and pollution, resulting in changes in local and global climate. These climate variabilities are further expected to alleviate in the future, contributing to frequent climate extremes. The frequent occurrence and intensity of extreme events such as storms, typhoons, particularly during weather events lead to crop failure, flash flooding, thereby threatening habitats, and loss of human lives. Irregular and untimely precipitation patterns, quite common in the region, leads to huge stress on water-supply, crop losses, resulting in prolonged droughts.

2.2. Drought: The Concept

Drought is among the most expensive weather-related disasters in the world, having major impacts on food security, and famines in different parts of the world (Pandey et al., 2007). Global climate change associated with drought affects temperature, precipitation, with increasing the rate of evaporation and transpiration. This recurring, natural condition doesn't have one universally accepted definition. The World Meteorological Organization (WMO) however termed drought as the period of below average precipitation for a prolonged period of time, resulting in a shortage of water and extensive damage to crops. The definition of drought also varies with regions, for example, a drought in Africa may not have the same definition in North America. Generally, the definition of droughts can be described as the occurrence of a rare, random, long-term phenomenon of dry conditions, prevailing from months to years by having a substantial effect on the water stress of a region (Zhang et al., 2017). Drought is often characterized on the basis of severity, duration, location, and timing, grouped into four perspectives- (a) meteorological; (b) agricultural; (c) hydrological; (d) socioeconomic (Mehran et al., 2016). Meteorological drought can be defined on the basis of the climatic conditions of a particular region, such as the degree and duration of the dry period, as a result of precipitation deficit. The meteorological drought is followed by agricultural and hydrological drought, which results from the impacts of meteorological drought (Drought Assessment and Forecasting, WMO 2005). Agricultural drought can be associated with the soil water deficit required for a crop, whereas hydrological drought considers the frequency and severity of precipitation shortages on surface, sub-surface (groundwater) water bodies. Socioeconomic drought is associated with the actual availability (supply and demand) of water to the people, which is more prevalent in under-developed countries. The environmental factors, such as land degradation, loss of biodiversity, in combination with economic impacts, like loss of crop

and livestock production, together have a larger impact. Apart from economic, social, and environmental impacts, droughts impact the health of human beings by increasing morbidity and loss of life. In recent years, the impact of drought has impacted the lives of one billion people (CRED and UNISDR, 2015). There has been an unprecedented increase in the occurrence of moderate to extreme drought events in the past 50 years in every continent (Mishra and Singh., 2010). Due to the intrinsic nature and complexity of drought, there are only few drought warning and prediction systems available for identification and characterization of the duration, severity, and spatial extent of drought (Grasso et al., 2011). Despite several advancements in drought analysis, the assessment of drought parameters is very critical in this risk-based paradigm. The lack of continuous spatial coverage data and limited measurements in existing observational networks for in-situ drought monitoring has paved a new way, towards the use of satellite data through remote sensing. The satellite-based sensors, such as Moderate Resolution Imaging Spectroradiometer (MODIS), Tropical Rainfall Measuring Mission (TRMM), Gravity Recovery and Climate Experiment (GRACE), collect global data across the visible, infrared, microwave portions of the electromagnetic spectrum at varying spatial resolutions, providing information on different components of the water cycle. A comprehensive approach of integrating precipitation, streamflow, soil moisture, temperature into a composite drought indicator can be helpful in monitoring and predicting the current and potentially changing drought patterns. The use of existing remote-sensing based drought indices has become popular because of the availability of information on drought conditions in areas where in-situ data are not available. To quantify the drought severity parameters, a combination of the remote sensing-based index, Land Surface Temperature (LST), and/or precipitation data is often used (Rhee et al., 2010). The indices are the numerical representation of drought severity derived from large hydroclimatic data, which

provides the overall qualitative state of drought (Ntale and Gan., 2003). The derived drought severity measures like Palmer Drought Severity Measures (PDSI) (PDSI; Palmer, 1965), Standardized Precipitation Index (SPI) (SPI; McKee et al., 1993, McKee et al., 1995) are the most commonly used drought indices globally. Other popular drought indices include Surface Water Supply Index (SWSI), Normalized Difference Drought Index (NDDI), Palmer Hydrological Drought Index (PHDI), Soil Moisture Deficit Index (SMDI). World Meteorological Organization (WMO) and NHMSs recommended SPI as the standard index for monitoring meteorological drought, while indices like SWSI and NDVI are used extensively for addressing hydrological and agricultural drought respectively (Hayes et al., 2011). SPI is also used for characterization of hydrological drought in areas, which lack streamflow data, but it doesn't quantify the temporary storage of precipitation and snow deficit (Staudinger et al., 2014). Makokha et al., 2016 accounted for the characteristics of snow and glacier (e.g. amount of water after the melting of snow) to understand the accurate water availability in cold regions for quantitative hydrologic drought monitoring. The Normalized Difference Vegetation Index (NDVI) is one of the popular, commonly-used remote-sensing based vegetation index for drought monitoring for identifying the extent of changes in vegetation cover and occurrence of drought (Sruthi and Aslam., 2015). Son et al., 2012 used MODIS NDVI and LST for monitoring moderate to severe drought across LMB, with extreme severity over Cambodia and Thailand. Drought indices are mostly used for classifying the type of drought, by determining the severity, duration, timing, and location of drought events. While the use of a specific drought index doesn't help in the precise prediction of drought characteristics, a combination of multiple drought indices can provide a better representation of different complexities of drought (Sun et al., 2012). Rhee et al., 2010 used the Scaled Drought Condition Index (SDCI), a combination of NDVI, LST, and precipitation data, for

monitoring drought in an arid, and humid region in the United States, which performed phenomenal, in accordance with the real drought occurrence. Gu et al., (2007) showed a better assessment of drought over grassland using the (Normalized Difference Drought Index) NDDI index in combination with the NDVI and NDWI.

With rapid population and economic growth, Southeast Asia has emerged as one of the fastest developing regions in recent decades. The significant growth of the region comes from a series of economic reforms due to strong regional cooperation, technological advancements, and resilient domestic consumption (Source: Economic Outlook for Southeast Asia, China, and India, 2018). Though agriculture remains the dominant sector for economic growth in most of the Southeast Asian countries, a steady progress to industrial and service sectors has been evident in recent times. Thailand and Vietnam have witnessed a major shift from predominant agrarian economies to more commercialized agriculture and industrialized economies. The Mekong River plays a crucial role in the region's development, from navigation and agriculture to the world's most productive inland fishery, serving as a lifeline for the rural communities of Cambodia, Lao, and Vietnam. Majority of the region's economy comes from agriculture and fisheries, especially rice and rubber. Other common crops in the region include coffee, cassava, soybean, maize, and sugarcane. Strong urbanization also increases the prospects of higher hydropower potential to meet the energy needs of the region, resulting in several hydropower projects since last 10 years. The hydropower potential of Mekong is estimated to increase by 7 percent from 2010 until 2020 (Mekong River Commission, 2010). With the recent pace of development in the Lower Mekong economies, there has been huge alterations in the region's land cover, oceans, climate systems, and other biogeochemical processes, resulting in an increase of extreme events. There have been several pieces of evidence of an increase in temperature in the LMB countries, resulting in the periodic

occurrence of natural calamities, such as cyclones, floods, droughts (Christiansen et al., 2007). The significant shift of forest land coverage to an increasing agricultural and vegetation land-use has resulted in changes of the seasonal water yield, groundwater recharge, evapotranspiration rates and rainfall patterns (Bruijnzeel., 2004, Brown et al., 2005). The recent construction of dams in the riparian neighbor's Lao, Cambodia, Thailand has also led to widespread concerns about the impacts on the natural eco-system. The existing dams in China have started impacting the lower stretches of the Mekong River, by changing the river's hydrology, which has led to a reduction in fish populations and alterations of the natural flow patterns, trapping much of the essential sediment-rich nutrients by converting large portions of the river into reservoirs (Pokhrel et al., 2018). Drought has been the most frequent event over LMB countries in the last three decades, with major events in 1992-1993, 1998-1999, 2003-2005 and 2010-2011 (Guo et al., 2017; Hundertmark., 2008). The four countries faced the worst prolonged drought from late 2015 through July 2016, causing huge losses in the agricultural sector alone. The damages from flood and drought in Cambodia between 1997-2001 accounted for 90 percent of all climate-related hazards, resulting in a shortage of agricultural land due to flooding (Asian Disaster Preparedness Center, 2002, Ministry of Environment, 2001). These events have led to irregularities in the hydrologic cycle, such as heavy, untimely distribution of precipitation, increasing the number of warm days, thus posing a challenge for efficient management of water resources and agricultural productivity.

2.3. Overview of the Cropping Sector

About half of the world's population are dependent on rice as their principal source of nutrient, with Asia housing 91 percent of the global production (Sawano et al., 2008; FAO 2002). The LMB is considered among the agricultural productive regions of the world, with over 10 million hectares

of cultivated land for rice production (MRC, 2014). Vietnam holds the tag for largest producer of rice, with 4.86 t/ha, followed by Lao (3.28 t/ha), and Cambodia (2.16 t/ha) between 1993-2004 (Kirby and Mainuddin 2009), with Thailand and Vietnam accounting for 50 percent of the global rice exports (Steudto et al., 2009). Majority of the rice cultivation throughout the Mekong basin are rain-fed, except the deltaic regions of Vietnam (Pokhrel et al., 2018). The productivity in the basin varies from location depending on climate, crop management (irrigation type and management practices), physical conditions (topography), availability of water, and soil type of the region, with Cambodia and Northeast Thailand having the lowest productivity in contrast with the deltaic regions of Vietnam. The structural transformation of the LMB economy has resulted from the profound increase in agricultural productivity, with a majority of the population actively engaged in this sector (MRC, 2010). About 10 million hectare of upland rice and 13 million hectares of lowland rice are affected by abiotic stresses, such as water-deficit (drought) or excessive watering (flooding/ water-logging). The water stresses are even further aggravated by the changes in local precipitation and temperature patterns. Rice production plays a crucial role in the agricultural sector and the livelihood of the farmers. More than 55 percent of rain-fed rice is produced in Southeast Asia (source: Foreign Agricultural Service, USDA). The projected rice yield for Vietnam, Thailand, Lao, and Cambodia are presented in Table 1. The rice yield in these riparian countries has seen an upward trend, in terms of production and demand, with the future yield estimates expected to double by 2050 (Figure 1). The yield projections were based on the trend curves in the crop yield of 1990-2012, obtained from FAOSTAT. The projected rice yield is expected to increase considerably higher than the present amount if historical trends continue. The current rice yields of Cambodia are less than the neighboring LMB countries, with Vietnam and Thailand responsible for 50 percent of the world's export. The projected yield estimates for rice

Table 1. Country wise projected yield of rice in 2025 and 2050 over Lower Mekong region

(source: MRC, 2014)

Country	Projected Yield in 2025 (in %)	Projected Yield in 2050 (in %)
Vietnam	19.01	60.56
Thailand	24.57	62.86
Lao PDR	32.25	84.19
Cambodia	34.85	102.53

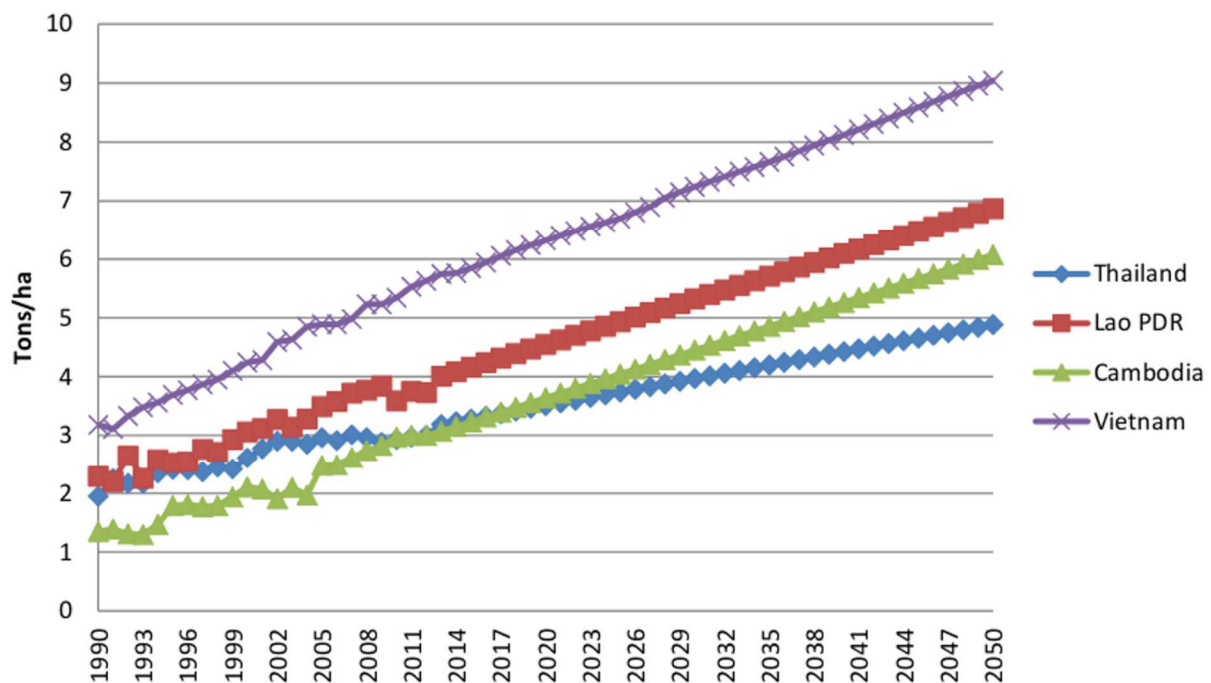


Figure 1. Actual (1990-2012) and projected rice yield in LMB for 2025 and 2050 under climate

change. (source: MRC, 2014)

can be only be achieved by improving the management practices, like increasing the application of pesticides, mechanization of farming systems, and use of genetically advanced rice varieties (high yielding cultivars). The rate of fertilizer application plays a crucial role in promoting crop growth and improving agricultural productivity. So, recognizing the growing impacts of climate change on agriculture and water resources, an urgent need for minimizing the risks associated with

food security and the environment is necessary. This study presents a drought monitoring system for capturing the probabilistic drought information based on multiple drought indicators.

2.4. RHEAS: Software Description

The incorporation of earth observation data and satellite data into a drought and crop monitoring system was implemented at the Lower Mekong Basin to understand the regional and national environmental conditions related to hydrology and crop yield. A remote sensing constrained, modeling framework, Regional Hydrologic Extremes Assessment System (RHEAS), was used for hydrologic modeling, and monitoring drought and crop yield. RHEAS was developed at NASA's Jet Propulsion Laboratory and implemented in the SERVIR hub at ADPC in Bangkok, Thailand. The implementation of RHEAS at the Lower Mekong Basin was intended to support climate resilience studies in the region. The main component of the RHEAS architecture consists of a spatially enabled relational database (PostGIS), which ingests a suite of model datasets and

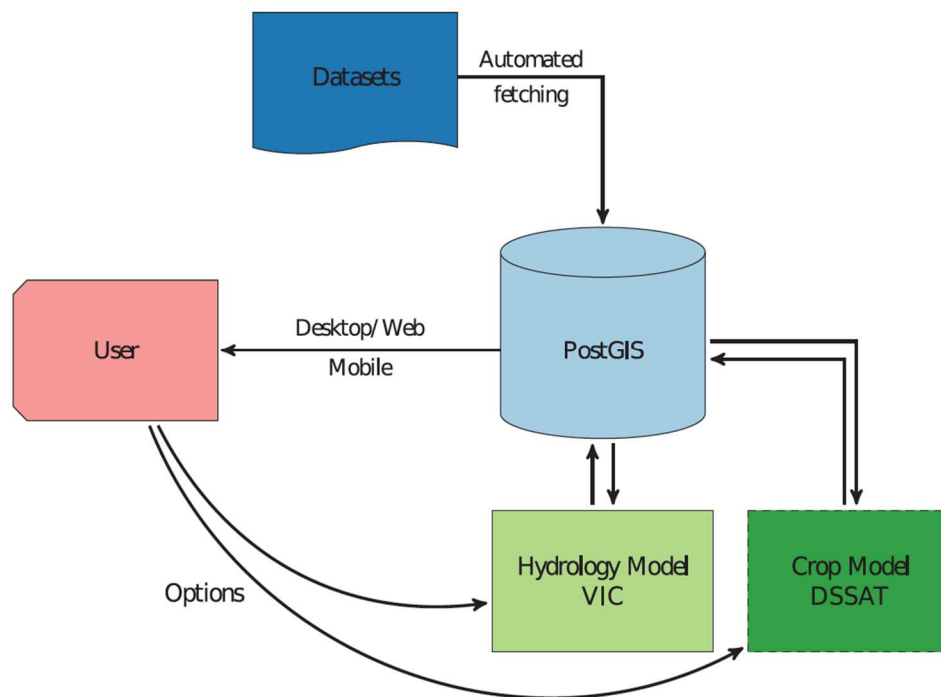


Figure 2. Schematic view of the Regional Hydrological Extremes Assessment Systems (RHEAS) framework

satellite observations, including meteorological data, and in-situ observations. Figure 2. illustrates the RHEAS software architecture, along with its components. RHEAS integrate meteorological inputs from model simulations and remote sensing observations for monitoring drought and crop yield. All the datasets required for model simulation, along with outputs are automatically fetched and stored in the GIS-enabled database. The missing datasets, including satellite observations, that are not produced by RHEAS are also automatically ingested into the PostGIS database. The advantage of such design is helpful to better facilitate transferability of data across models, and the ability to perform spatial operations and complex queries via GIS interface. Additional information about RHEAS can be obtained from the NASA/RHEAS webpage (<https://github.com/nasa/RHEAS>). Figure 3 presents the schematic of the RHEAS algorithm, with both nowcast and forecast modes of operation. Precipitation and other data products, required for the model simulations, are either available from in-situ datasets or satellite sensors via remote

Figure 3. Schematic view of the RHEAS algorithm with remotely sensed datasets to provide hydro-climatic states and indicators

sensing. The development of remote sensing techniques has led to the availability of continuous, finer scale data on different hydrologic components of the water cycle, from satellite sensors, such as Climate Hazards Group Infrared Precipitation with Station data (CHIRPS), Moderate Resolution Imaging Spectroradiometer (MODIS), Tropical Rainfall Measuring Mission (TRMM), Gravity Recovery and Climate Experiment (GRACE), Soil Moisture Active Passive (SMAP). A hindcast study at the NASA SERVIR hub at RCMRD in Nairobi, Kenya was conducted for drought monitoring and seasonal forecast of maize yield over East Africa (Das et al., submitted). The current implementation of RHEAS is at a spatial resolution of 25 km, that is initialized daily, providing nowcast products. The datasets available in RHEAS database comprise of different components of the hydrologic cycle, such as precipitation, evapotranspiration, temperature. Table 2. shows a list of available data products in RHEAS, along with their spatial and temporal resolution.

RHEAS consist of a hydrological model, coupled with a crop model to provide the current linked hydrologic and yield assessments. The Variable Infiltration Capacity (VIC) (VIC: Liang et al., 1994; Liang et al., 1996) hydrologic model was deployed in RHEAS to simulate soil moisture and streamflow from daily weather data using GIS. VIC is a large-scale, semi-distributed hydrologic model that solves full energy water balance over a gridded domain. The detailed description of the VIC model is presented in Chapter 4. Several studies by Sheffield et al (2006), Sheffield and Wood, (2007), Zhao et al, (2011), Shukla et al, (2013), Nijssen et al, (2014) have successfully used VIC for monitoring watershed hydrology and drought conditions across a range of varying hydro-climates. Many process updates of the model, such as snow model updates (Andreadis et al., 2009), cold land processes updates (Cherkauer et al., 2003), dynamic lake and wetland model (Bowling and Lettenmaier., 2010), has been performed in the previous studies. VIC has been widely used

for seasonal flow forecast, water stress, and climate resilience studies. The implementation of RHEAS using VIC for assessing drought conditions has been performed over East Africa (Das et al., submitted; Andreadis et al., 2017).

Table 2. Available datasets in the RHEAS database along with spatial and temporal resolution

Variable	Product	Spatial Resolution	Temporal Resolution	Duration of Data Availability
Precipitation	CHIRPS	5 km	Daily	1981-Present
	TRMM	0.25°	Daily	1998-2014
	PRISM	4 km	Daily	1981-Present
	GPM	0.1°	Daily	2014-Present
	CMORPH	8 km	Daily	1998-Present
	Princeton	0.25°	Daily	1948-Present
	RFE2	25 km	Daily	2000-Present
Wind Speed	NCEP	1.875°	Daily	1948-Present
	Princeton	0.25°	Daily	1948-Present
Temperature	Princeton	0.25°	Daily	1948-Present
	NCEP	1.875°	Daily	1948-Present
	PRISM	4 km	Daily	1981-Present
Soil Moisture	SMAP	36 km	Daily	2015-Present
	SMOS	40 km	Daily	2009-Present
	AMSR-E	25 km	Daily	2002-2011
Evapotranspiration	MOD16	1 km	8 Days	2000-2013
Water Storage	GRACE	300 km	Monthly	2002-Present
Leaf Area Index	MCD15	1 km	8 Days	2002-Present
Meteorological Forecasts	IRI	2.5°	Monthly	2000-Present
	NMME	0.5°	Daily	2000-Present

(Source: Andreadis et al., 2017)

The Decision Support System for Agrotechnology Transfer DSSAT/CERES-Rice model (Jones et al., 2003), developed by the International Benchmark Systems Network for Agrotechnology Transfer, was used as a crop model for the simulation of growth, development, and yield under given management practices and soil properties. A considerable amount of studies using DSSAT has been performed by Hoang et al., (2016), Sarkar and Kar., (2008), Jiang and Jin, (2009) for assessing the potential impacts of climate change on agriculture. The datasets required for the simulation of DSSAT include cultivar information (types of cultivar used), planting start date, soil

properties, which are stored in the schema in the form of tables and raster maps. The soil information is essential for the simulation of soil water balance and crop growth. The RHEAS-DSSAT model in the RHEAS framework is a modified version of the baseline DSSAT model, which could stop and re-start at arbitrary times, unlike other crop models, that tend to run continuously from sowing until harvest (Ines et al., 2013). The output of RHEAS includes a large range of hydrologic variables (runoff, soil moisture), and derived drought severity measures (SPI, PDSI), linked directly to agricultural crop yield at 25 km resolution. RHEAS use the available data (like precipitation) from satellite observations and/or model outputs to provide with maps and information products of drought severity measures (SPI, Drought Severity) in nowcasting mode of operation (Steinemann and Cavalcanti., 2006; Mu et al., 2013).

Chapter 3.

SITE DESCRIPTION

3.1. Location and Description

Being the seventh largest river in Asia, the Lower Mekong river forms an integral part in the lives of the 60 million people residing in the four countries of Lao PDR, Cambodia, Thailand, and Vietnam (Ziv et al., 2012; MRC 2010). With a densely rural populated area, there is a substantial reliance of the community on the river for their livelihood, with agriculture and fishing as the major lifeline for the local people. The region is rich in aquatic biodiversity, ethnicity, and cultures. The LMB has two dominant seasons- wet south-west monsoon (May-Oct), and dry north-east monsoon (Nov-April) (Kite., 2001). The LMB gets more than 85 percent of the precipitation in the wet season, from mid-May until October, and the north-east monsoon in dry season bearing minimal precipitation (MRC 2011). In addition to the southwest monsoon from the Bay of Bengal and northeast monsoon from Pacific, some studies have argued about the complex monsoon geography. According to a study by Wang & Lin, the Mekong countries are affected by the South East Asia Monsoon, North East Pacific Monsoon, and Indian Summer Monsoon. Rice is the primary crop grown in the region, with over 10 million hectares of Lower Mekong Basin used for rice cultivation. The amount of rice grown in the four countries are disparate, depending on the topography, climate, location of the Mekong river, and agricultural practices in the area. About 3.5 million hectares and 1.5 million hectares of the area are used for irrigation in the wet and dry season respectively. The basin is characterized by its complex varying topography, climate, and biodiversity.

3.1.1. Topography and land-use

The landscape and climate in the area differ in the four countries depending on the location of the

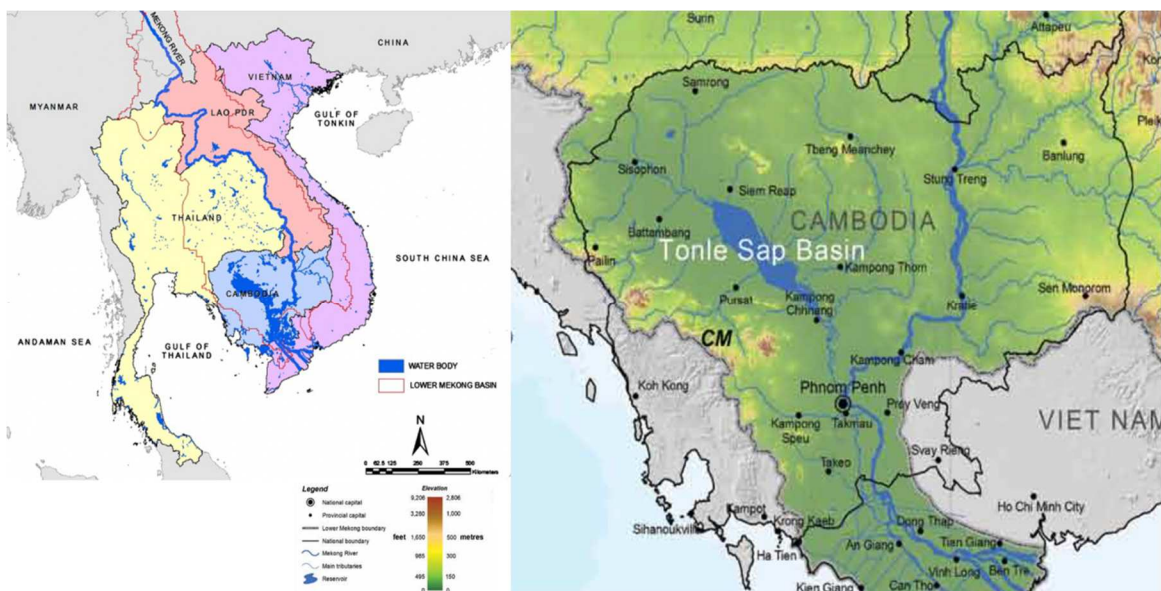


Figure 4. Map of the Mekong River Basin (top); Location of the four countries in Lower Mekong Basin (bottom left); Elevation map of the study area: Cambodia (bottom right)

river, ranging from steep, rugged, mountainous topography of Lao to the low-level deltaic plains of Vietnam. Figure 5. shows the land cover pattern over Cambodia. Majority of the land is used

for paddy cultivation (yellow color represents paddy plantation in Figure 5.) along the Tonle Sap floodplains. The north and northeast portion of Cambodia are mostly covered with deciduous forests, with some areas used for cash crop plantation. Most of the high elevation areas are covered with evergreen forests, mostly suitable for swidden agriculture. The southern uplands also consist of mountains, with heavy rainfall and little scope for agriculture. The deltas within the basin, Tonle Sap floodplain, and the low-lying Mekong plains, commonly referred as the “Rice bowls of Asia”, house over a third of the population in the area, with a total annual production of rice exceeding 46 million tonnes. The Tonle Sap basin is an important part of the Lower Mekong, with most of the agricultural productive areas around the basin. The cropping pattern in the basin varies from places, with differences in the area for plantation in the growing seasons.

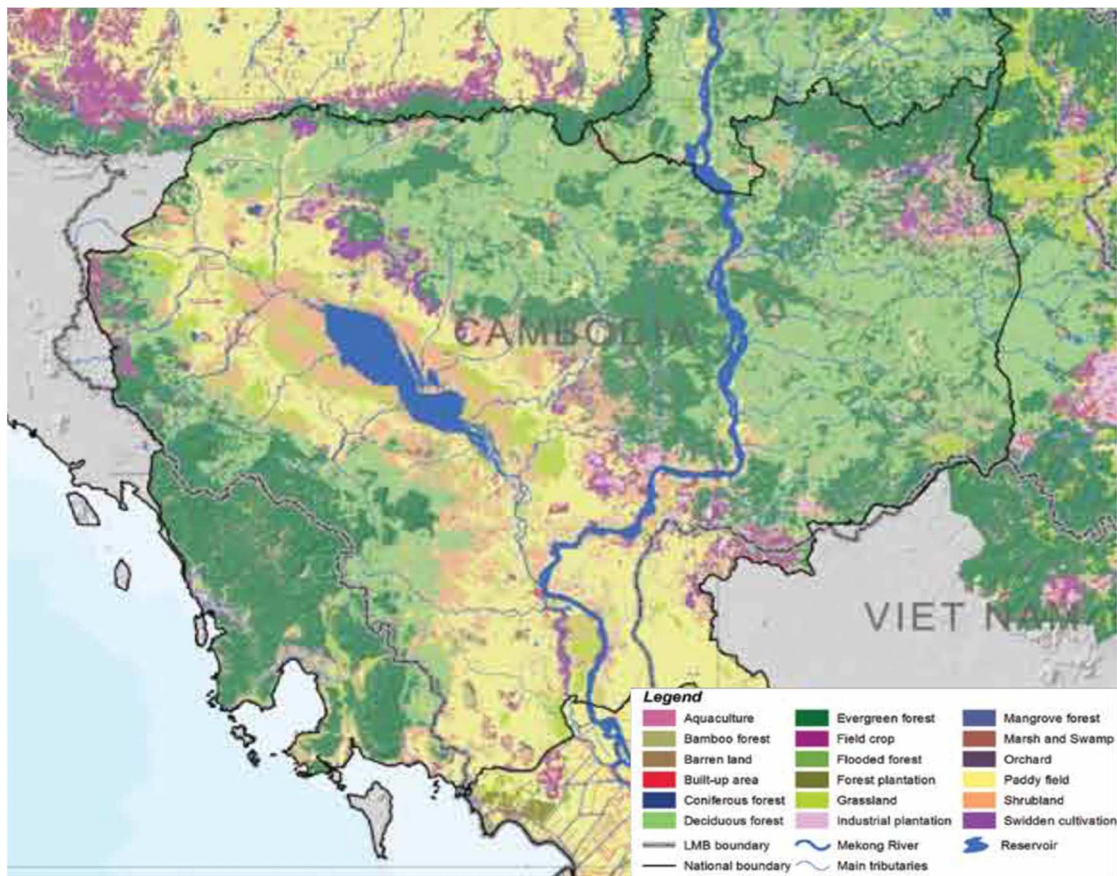


Figure 5. Land-use pattern over Cambodia

3.1.2. Geology

The Mekong River has a constrained bedrock or old alluvium geology in the bed and riverbanks. The plateau comprising Northeast Thailand and parts of Lao basin have an underlying salt deposit, with a variable thick alluvium surface covering the basin in Cambodia (Gupta, 2009). These areas have been the most affected by floods, due to extensive deforestation in recent years.

3.1.3. Hydroclimate

The variability of rainfall in the basin is distinctive, with western slopes of Annamites of Lao and Vietnam, getting more than 2,500 mm of annual rainfall per year in contrast with the Northeastern portion of the delta and Thailand, that experiences a mean annual rainfall of less than 1,200 mm per year. Some portions of the basin, like west of Laos and Vietnam, are highly productive because of the high amount of precipitation in both seasons. The variation of temperature throughout the basin can be observed with a change in elevation, ranging from 22-28°C and evaporation rates of 1,000-2,000 mm per year.

3.1.4. Biodiversity

The LMB has one of the richest areas of biodiversity, with about 20,000 plant species and 850 species of aquatic life. With over 100 different ethnic groups, the region reflects the diversity of the natural ecosystem. About 85 percent of the population depend on their livelihood from the river basin's resources (fish and water).

3.1.5. Socioeconomic conditions

The basin serves the people in different ways, depending on the location and accessibility of the river. Water for agriculture, fish farming, and transport routes are some of the important sources for the local communities. The Mekong has the second highest aquatic biodiversity in the world

after the Amazon. About 50-80 percent of protein intake for the communities, especially rural people who are highly dependent on the river, comes from fish and other aquatic products.

3.1.6. Navigation

The river makes an important travel-way for local and international trades, linking communities through the exchange of goods like timber, agricultural products. The river also links the neighboring countries, enabling the exchange of goods to boost the economy. The waterborne trade between the Mekong countries has increased significantly in recent times, which have led to a number of agreements between the countries to enable trade and passage.

This highlights the importance of water resources in LMB for people and ecosystem services, and any water resources constraints would jeopardize the human life and natural resources in this region. To mitigate these water resources constraints, this study was implemented in Cambodia, as a representative of the LMB, to monitor the effects of drought on rice production.

Chapter 4.

DATA AND METHODS

4.1. Setting up the model

RHEAS is an integrated software framework comprising of a hydrologic model and crop model that monitors the water stress, drought parameters, and expected crop yield. The installation of RHEAS requires a number of python packages (NetCDF4, GDAL, Scipy), a GCC compiler for creating, assembling and deploying the required applications (<https://github.com/nasa/RHEAS>). After installation of the necessary software packages, a PostgreSQL server along with the PostGIS extension is installed by running the Buildout script. The PostgreSQL is an open source object-relational database system that uses and extends the SQL language combined with many features for managing data stored in relations (tables) (Obe et al., 2015). The Buildout tool is used for automating the software assembly for generating configuration files and scripts. It also creates a database for the user and builds the hydrology model. The database stores the necessary information to run the system including model datasets (input and output), satellite data products, and in-situ observations. This functionality of RHEAS allows the hydrologic and crop model to interface with the database, rather interaction with the internal formats of the model. Thus, allowing for better transferability of data between the constituent models.

4.2. Data Acquisition

RHEAS have a set of available data products (Table 2) along with their spatial and temporal resolution, and duration, each variable representing a component of the water cycle. The data ingestion and simulations in RHEAS are performed through a simple text-based configuration file. The 'data' configuration file is used to provide information about the datasets required for model simulations, by specifying a bounding box over the area of interest (i.e. latitude and longitude),

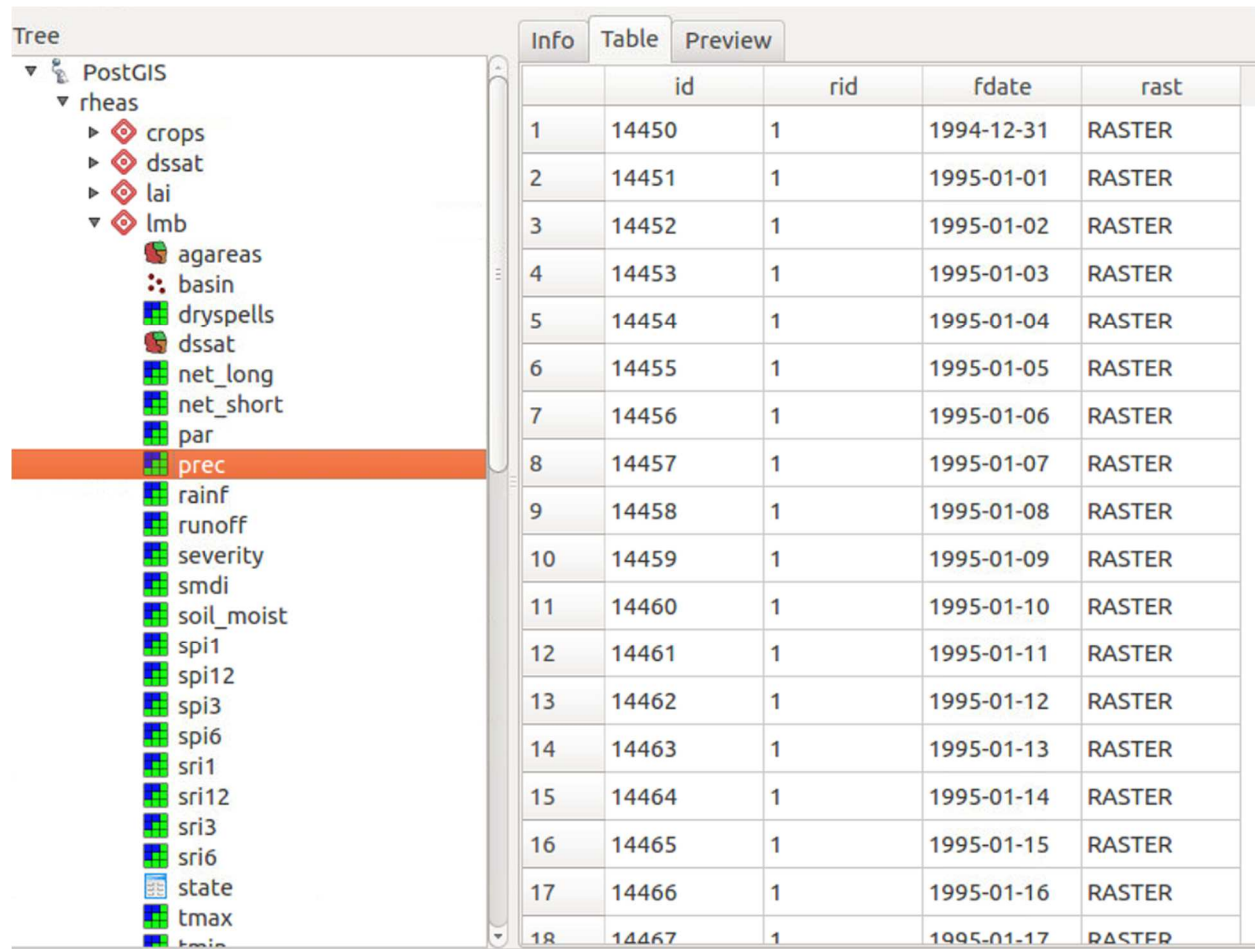
along with the name of the datasets, and duration of data. Figure 6. illustrates a typical data configuration file with the specified datasets. The spatial extent of datasets to be ingested is done

```
1  
2      [domain]  
3      minlat: 8.00  
4      maxlat: 24.00  
5      minlon: 101.00  
6      maxlon: 110.00  
7  
8      [chirps]  
9      startdate: 2014-01-01  
10     enddate: 2015-12-31  
11  
12     [ncep]  
13     startdate: 2014-01-01  
14     enddate: 2015-12-31  
15  
16
```

Figure 6. A typical Data Configuration File, providing the dimensions of the study area, along with the source and duration of the ingested datasets

by creating a model domain over the study region, by specifying the minimum and maximum longitude and latitude, along with the duration of the dataset. The domain represents the geographical area for which the datasets for model simulations will be ingested into the database. The database in RHEAS consists of datasets, grouped into schemas, each representing a particular variable. For example, the precipitation, temperature, wind speed related variables are contained in three different schemas- 'precip' (precipitation), 'tmax' and 'tmin' (temperature), 'wind' (windspeed). Similarly, the hydrological and crop model parameters are available under the 'vic' and 'dssat' schemas. These schemas consist of different tables, for example the 'vic' schema consists of the soil parameters, while the 'dssat' schema contains information about cultivars and soil properties. All the variables stored in a table have a spatial and temporal dimension, constituting of a unique id, date, data type (e.g. raster), and geometry of the area. The raster data types are partitioned into tiles, each representing the value of a variable (e.g. precipitation, severity)

for a particular date. Figure 7. shows a sample of a precipitation table inside the 'prec' schema. Similarly, for other variables, the table assigned stores the daily values, either as a raster or polygon. Precipitation is the most important variable in hydrologic modeling, with air temperature



	id	rid	fdate	rast
1	14450	1	1994-12-31	RASTER
2	14451	1	1995-01-01	RASTER
3	14452	1	1995-01-02	RASTER
4	14453	1	1995-01-03	RASTER
5	14454	1	1995-01-04	RASTER
6	14455	1	1995-01-05	RASTER
7	14456	1	1995-01-06	RASTER
8	14457	1	1995-01-07	RASTER
9	14458	1	1995-01-08	RASTER
10	14459	1	1995-01-09	RASTER
11	14460	1	1995-01-10	RASTER
12	14461	1	1995-01-11	RASTER
13	14462	1	1995-01-12	RASTER
14	14463	1	1995-01-13	RASTER
15	14464	1	1995-01-14	RASTER
16	14465	1	1995-01-15	RASTER
17	14466	1	1995-01-16	RASTER
18	14467	1	1995-01-17	RASTER

Figure 7. Precipitation values for each day in the 'prec' table of 'lmb' schema stored as raster in RHEAS database

and wind speed as additional requirements. The high-resolution (0.05°) daily historical precipitation record from Climate Hazards Group Infrared Precipitation with Station data (CHIRPS), starting 1981 to near-present was used to create a gridded time series for trend analysis and drought monitoring (Funk et al., 2015). The long-term daily precipitation data is collected

from satellite imagery and a range of weather stations globally. Other input requirements and source of data for the hydrologic and crop model simulations are discussed in the subsequent sections.

4.3. Methodology

4.3.1. Hydrologic Modeling

The Variable Infiltration Capacity (VIC) (Liang et al., 1994) model was used to simulate the land-atmosphere fluxes and the water and energy balances at the land surface at a daily time-step. In this study, the VIC model was used to simulate soil moisture and runoff/streamflow over Cambodia. The land surface model partitions the land surface into flat, uniform grid cells of 0.25 degree, with no communication between the cells (i.e. every cell is considered as independent). Vertical movement of water is only allowed into a grid cell, with no non-channel flow between grid cells. Based on the canopy resistance and LAI, the land cover types are specified and grouped into land cover classes. For example, a land cover (e.g. forest, grassland) of the same type are classified into one tile, which is then averaged together (weighted by area fraction) to give the grid-cell average of the fluxes. The model characterizes the sub-surface into three soil layers and a single canopy layer on top with the vertical movement of water modeled as gravity drainage (Liang et al., 1994; Sheffield et al., 2004). Later on, Liang et al (1996) suggested the improvement of evapotranspiration predictions with the addition of a third soil layer. Figure 8. presents a schematic of the variable infiltration capacity (VIC) macroscale hydrologic model. Based on the Penman-Monteith equation, the evapotranspiration over each grid cell is computed by summing the evaporation from bare soil and transpiration from vegetation, weighted by the surface area fractions (Liang et al., 1993). In this study, the routing of streamflow was not performed as horizontal flow into channels was not taken into account.

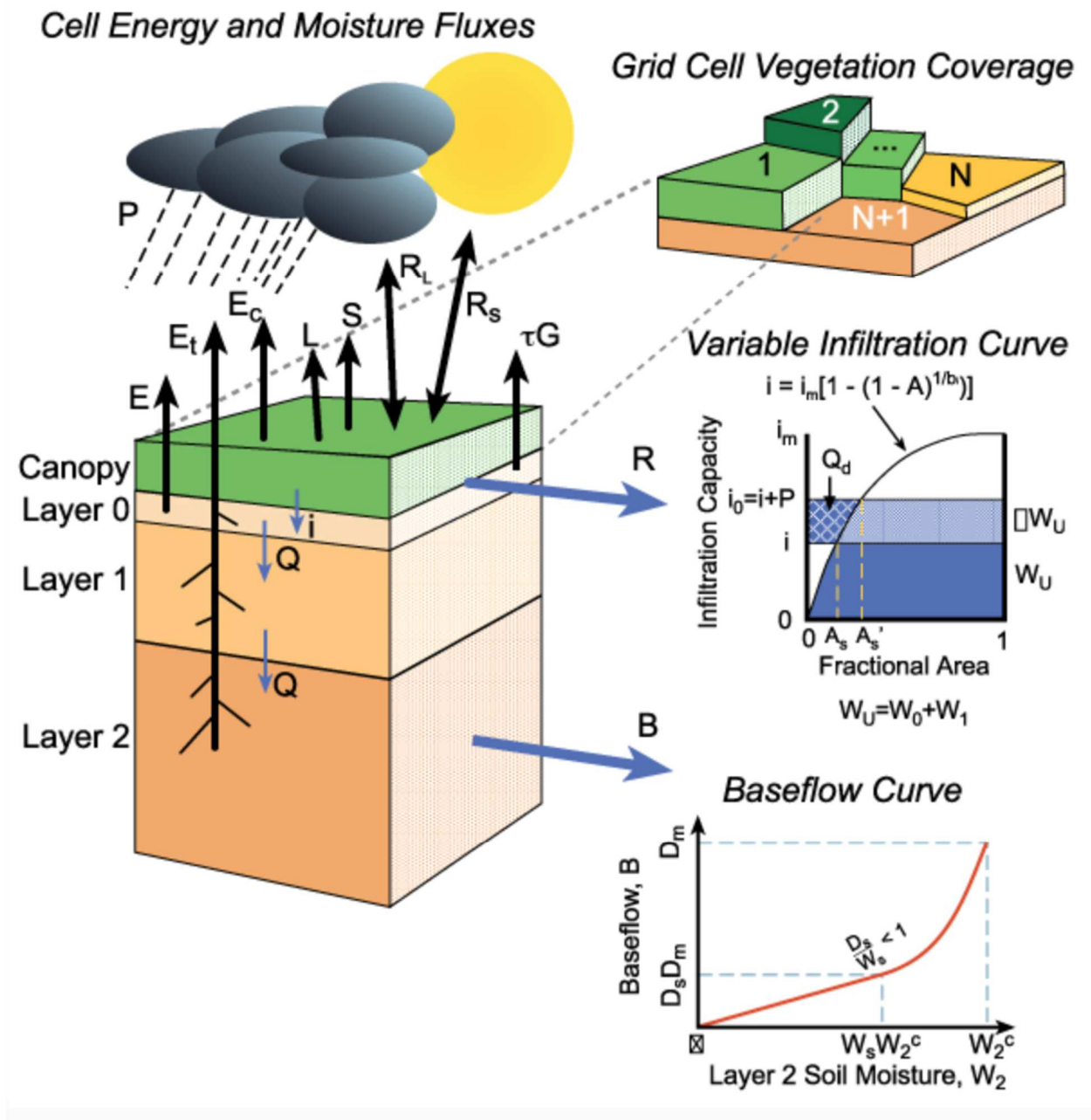


Figure 8. Schematic representation of the variable infiltration capacity (VIC) hydrological model (<http://www.hydro.washington.edu/Lettenmaier/Models/VIC>)

The minimum input requirements of VIC include meteorological forcing variables and daily time-series of land cover information. The meteorological input consists of the weather forcing such as

precipitation, air temperature, wind speed, longwave and shortwave radiation. In this study, the daily precipitation data from CHIRPS data product were evaluated over Cambodia for the period 2000-2018. The data constitutes of the precipitation value of a particular location at a given time. Other variables such as wind speed and air temperature were obtained by reanalysis from the National Centre for Environmental Prediction (NCEP) datasets (Kalnay et al., 1996). The topographic heterogeneity was modeled by dividing each grid cells into elevation zones, derived from the ~1 km spatial resolution GTOPO30 global digital elevation model. The fine resolution (500-m) Moderate Resolution Imaging Spectroradiometer (MODIS) global product provides information on land cover at annual time steps. The lack of grid-based soil information at the regional scale has been a major challenge in monitoring and modeling soil processes and understanding the interactions between land surface and the atmosphere (Arrouays et al., 2014). For the accurate simulations of the hydrologic and crop model, a high-resolution gridded soil database at 10 km resolution over Cambodia was used (Hengl et al., 2014). Using the meteorological data and land cover information, VIC explicitly generates the drought and hydrologic characteristics for each grid cell over the study domain. The primary drought severity measures such as SMDI, SPI, Dryspells, and hydrologic variables in terms of soil moisture, precipitation are some of the parameters generated by VIC. Based on the previous study by Komuscu., 1999, the SPI is calculated to quantify the frequency, duration and time scale, given as:

$$SPI = \frac{x_i - \bar{x}}{s}$$

where x_i is the monthly rainfall amount, \bar{x} is the mean of rainfall, and s is the standard deviation of rainfall calculated from the monthly values.

The Standardized Precipitation Index (SPI) is a normalized index calculated by the forcing of meteorological observations like precipitation, wind speed, and air temperature onto RHEAS for

effectively quantifying meteorological drought for multiple timescales, with shorter timescales representing the soil moisture and longer timescales representing streamflow, groundwater and reservoir effect. The SPI can be commonly calculated for 1,3,6,12,24 and 48-month timescales (Svoboda et al., 2012). RHEAS produce the 1,3,6 and 12-month SPI indices for each day of the entire simulation period. The observed precipitation data based on the long-term record for any location is fitted to a Gamma distribution, which is then transformed into a normal distribution (Edwards., 1997). Generally, the SPI value ranges from -2 to +2, indicating extreme dry to extreme wet conditions (McKee et al., 1993). A positive value indicates wet conditions (higher than median precipitation), while a negative SPI reflects dry conditions (lower than median precipitation). The drought intensities resulting from SPI in this study is based on Table 3.

Table 3. Meteorological conditions based on classification of standardized precipitation index (SPI) (source: McKee et al., 1993)

SPI Value	Meteorological Condition
≥ 2.0	Extremely Wet
1.5 to 1.99	Very Wet
1.0 to 1.49	Moderately Wet
-0.99 to 0.99	Near Normal
-1.0 to -1.49	Moderately Dry
-1.5 to -1.99	Severely Dry
≤ -2.0	Extremely Dry

The drought severity provides a standardized measurement of moisture conditions spatially over a period of time. Severity is derived from soil moisture values for each grid cell, where soil moisture for each grid cell is expressed as a percentile of the grid cell's model climatology. The severity gives an estimate of the relative dryness, while SPI quantifies the longevity of drought, by monitoring the impacts of precipitation deficit on soil moisture. RHEAS also compute the soil water deficit using the Soil Moisture Deficit Index (SMDI) to represent the available soil water in

the root zone (Narasimhan and Srinivasan., 2005). The weekly averaged soil water in the root zone and median of long-term available soil water was taken for computing the soil moisture deficit (in %). The moisture availability of soil in each week was given as follows:

$$SMDI_j = 0.5SMDI_{j-1} + \frac{SD_j}{50}$$

where $SMDI_{j-1}$ represents the SMDI of the time period (in weeks) over which the dryness value needs to be accumulated, and SD_j is the soil water deficit. The soil moisture deficit index is helpful for quantifying agricultural drought using the weekly soil moisture values. The SMDI values generally ranges from -4 to +4, with -4 indicating extreme dry conditions and +4 representing extreme wet conditions (Table 4). The SMDI is also calculated at various depths as the moisture content in the soil varies with depth depending on the potential of the crops to extract water.

Table 4. Meteorological conditions based on classification of Soil Moisture Deficit Index (SMDI)

(source: Narasimhan and Srinivasan., 2005)

SMDI Value	Meteorological State
3 to 4	Extremely Wet
2 to 3	Very Wet
1 to 2	Moderately Wet
1 to 0.5	Near-normal
0.5 to -0.5	Normal
-0.5 to -1	Near-normal
-1 to -2	Moderately Dry
-2 to -3	Severely Dry
-3 to -4	Extreme Dry

4.3.2. Crop Modeling

The system modularity of RHEAS allows the one-way coupling of the hydrologic model with other models in the system. The process-based Decision Support System for Agrotechnology Transfer (DSSAT) crop model was used in RHEAS for the simulation of crop growth, development, and yield under different management practices and soil properties. The DSSAT-

CSM-Rice model was adopted for simulating the phenological development of crops, and growth components from emergence until maturity (Jones et al., 2003). The minimum input requirements for DSSAT included time series of weather variables, fertilizer application rates, soil type, and cultivar-specific parameters. DSSAT uses the same soil information and weather forcing- rainfall, air temperature, net solar radiation, and relative humidity- as the hydrologic model. Other management information includes the crop variety and fertilizer practices. In this study, the simulations are performed for rice, the major crop grown in the region. The management data such as the rate of fertilizer application and types of cultivar were taken from published studies and reports. A short duration and medium duration rice cultivars from Cambodian Agricultural Research and Development Institute (CARDI) were analyzed for examining the potential rice yields in Cambodia. Genotype coefficients for both cultivars were taken from Ahn et al. (2017). Table 5. outlines the genotype coefficients for the two rice varieties used on the study, calculated with the GENCALC GC estimators. To promote crop growth and productiveness of plants, it is essential to supplement the required nutrients found naturally in the soil by modifying the soil conditions through the application of fertilizers. The fertilizer application rates give an idea about the nutrients used by the plants per unit area of arable land. Modern chemical fertilizer primarily includes Nitrogen, Phosphorus, and Potassium, or a combination of major nutrients, with minimal use of traditional nutrients such as plant and animal manure. The quantity of fertilizer for a particular crop depends on the variety of the crop. For instance, a long duration rice requires more fertilizer than a medium or short variety rice. Due to lack of information about the local management practices, the fertilizer (nitrogen) application rates in Cambodia were taken from the World Bank Data (Food and Agriculture Organization, electronic files and website). Figure 9.

shows the amount of nitrogenous fertilizers, commonly used in Cambodia from 2000-2017. For rice, fertilizer was applied in two to three splits, after 21 days of seeding and between 45-50 days

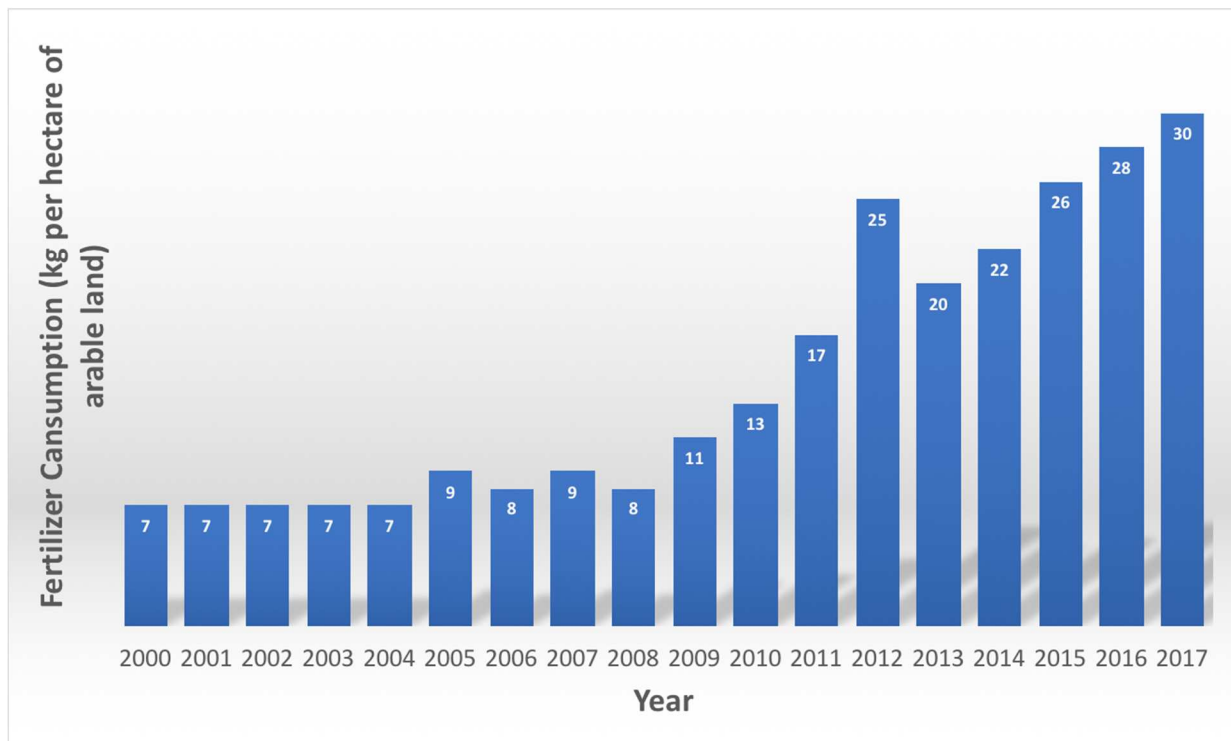
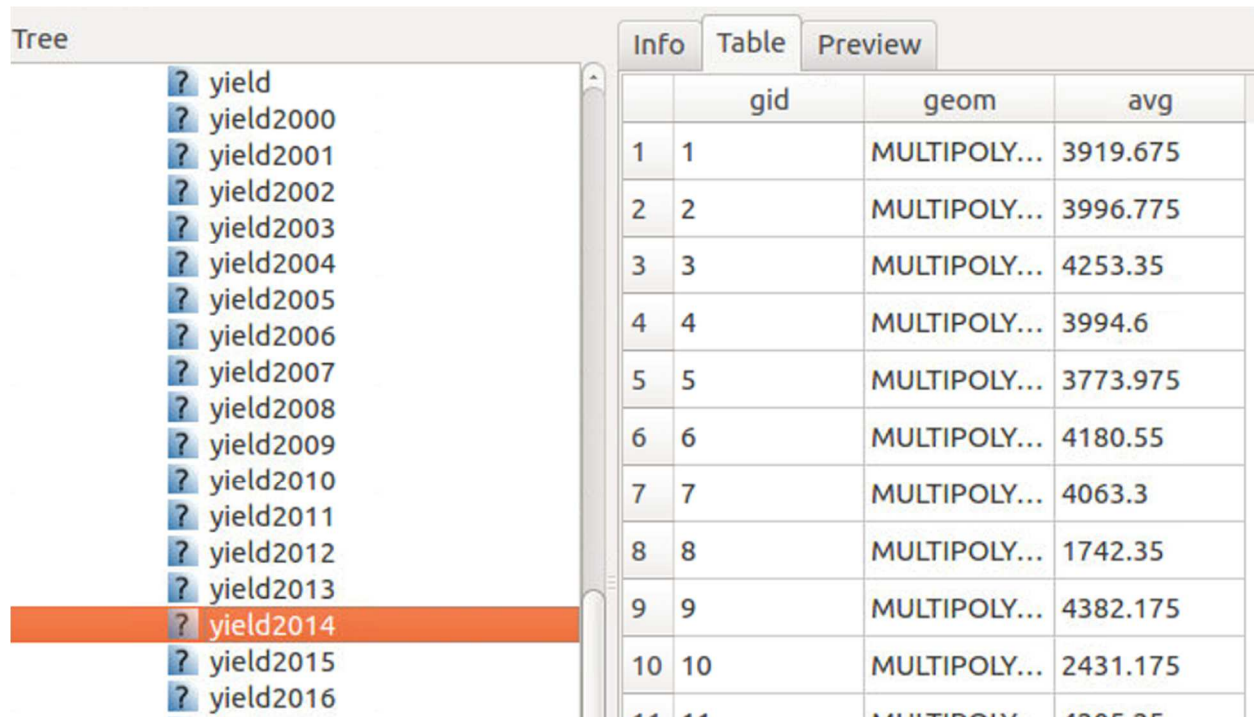


Figure 9. Fertilizer Consumption (kilograms per hectare of arable land) of Cambodia from 2000-2017

(panicle initiation) of seeding (Source: International Rice Research Institute). Cambodia is a poor economy, so the consumption of fertilizer and production of rice is very less compared to neighboring Thailand and Vietnam (largest producers and exporters of rice) (Kirby and Mainuddin 2009; MRC 2014; Steudto et al., 2009). A modified version of the DSSAT crop model was used in RHEAS, which could stop and re-start at arbitrary times unlike general crop models that run continuously from sowing until maturity (Ines et al., 2013). This modification will be helpful in future for assimilation of soil moisture and LAI observations during different phases of crop growth. Unlike the hydrologic variables that are stored as raster, the DSSAT computes the yield for every polygon in the shapefile. Thus, RHEAS give the yield estimates for each province

(computed as polygons) of Cambodia. Figure 10. illustrates a typical yield table of Cambodia, computed for each polygon.



Tree		Info	Table	Preview
?	yield			
?	yield2000			
?	yield2001			
?	yield2002			
?	yield2003			
?	yield2004			
?	yield2005			
?	yield2006			
?	yield2007			
?	yield2008			
?	yield2009			
?	yield2010			
?	yield2011			
?	yield2012			
?	yield2013			
?	yield2014			
?	yield2015			
?	yield2016			

	gid	geom	avg
1	1	MULTIPOLY...	3919.675
2	2	MULTIPOLY...	3996.775
3	3	MULTIPOLY...	4253.35
4	4	MULTIPOLY...	3994.6
5	5	MULTIPOLY...	3773.975
6	6	MULTIPOLY...	4180.55
7	7	MULTIPOLY...	4063.3
8	8	MULTIPOLY...	1742.35
9	9	MULTIPOLY...	4382.175
10	10	MULTIPOLY...	2431.175
11	11	MULTIPOLY...	4205.35

Figure 10. Sample Yield Table stored in a schema within the RHEAS database

4.3.3. Nowcast Simulations

RHEAS simulations were performed through a user-provided text-based configuration file that guides the model to perform the simulations by choosing the type of model- VIC or DSSAT. The RHEAS simulations can be performed either as single model realization or ensemble of models. Other than the mode of operation and choice of model, additional information such as the source of meteorological data, the period of simulation, the map of study area, the spatial resolution of the model, along with the input and output variables, are specified in the configuration file. Figure 11 shows a nowcast configuration file for the simulation of the hydrologic model.

```

1
2 [nowcast]
3 model: vic
4 startdate: 2000-01-01
5 enddate: 2000-12-31
6 basin: data/shapefile/Cambodia_ADM1.shp
7 name: lmb
8 resolution: 0.25
9
10 [vic]
11 precip: chirps
12 temperature: ncep
13 wind: ncep
14 save to: db
15 save state: SaveState
16 save: prec, soil_moist, tmax, tmin, net_short, net_long, rainf, drought
17 initialization: off
18
19 [dssat]
20 ensemble size: 40
21 shapefile: data/shapefile/Cambodia_ADM1.shp
22 assimilation: off
23 crop: rice
24
25

```

Figure 11. Nowcast Configuration File, showing the hydrologic simulation for Cambodia

VIC retrieves all the model inputs and stores the model simulations within the database, with additional details provided by the user through a configuration file. The hydrologic model is simulated over Cambodia from 2000 until 2017, with outputs stored as tables in a schema. The schema consists of tables of different hydrologic variables (e.g. soil moisture, runoff) and derived drought severity measures (e.g. SPI, severity) from the model run. Along with meteorological forcing (input to the hydrologic model), the options for saving the model state files and output variables (PostGIS database) are also provided in the configuration file. VIC also saves the hydrologic state from the previous simulation for specifying a start condition for the next model run. So, an option for the initialization of the model (on/off) from previously saved state file is provided during the hydrologic simulations. The model state guides the model to use the information from the previous run state file and re-start the simulation for the next run. A list of output variables saved from the model run, such as incoming precipitation, soil moisture content for each soil layer, rainfall, maximum and minimum temperature, the net downward longwave and

shortwave flux can also be specified in the configuration file. Similar to the hydrologic model, the DSSAT simulations are performed through the same configuration file after the hydrologic simulations, by providing information about the type of crop and map of the study area. The option for assimilation of soil moisture and LAI can also be provided during the simulation of crop model. No data assimilation was done in this study, rather stress was given towards the performance of the model with real scenarios.

Table 5. Genotype coefficients for two rice cultivars for Cambodia, used in the crop model

	Phenological coefficients				Growth Coefficients			
Rive Variety	P1	P2R	P5	P2O	G1	G2	G3	G4
Sen Pidao	554.400	87.7	251.100	13.00	68.67	0.021	1.00	1.15
Phka Rumduol	435.100	295.100	388.00	11.28	58.96	0.026	1.00	1.20

Phenology genetic coefficients

P1: Time period in °C (above a base temperature of 9 °C) from seedling emergence to the end of juvenile phase. Expressed as growing degree days (GDD)

P2R: Extent to which phase development leading to panicle initiation is delayed for each hour increase in photoperiod above P2O. Expressed as growing degree days (GDD)

P5: Time period from beginning of grain filling to physiological maturity with a base temperature of 9 °C. Unit: GDD

P2O: Critical photoperiod or the longest day length at which development occurs at a maximum rate. Expressed in hours

Growth genetic coefficients

G1: Potential spikelet number coefficients as estimated from the number of spikelets per g of main culm dry weight (less leaf blades and sheaths plus spikes) at anthesis. Unit: Spikelets per g of main culm

G2: Single grain weight under ideal growing conditions, i.e. non-limiting light, water, nutrients, and absence of pests and diseases. Expressed in grams

G3: Tillering coefficient (scalar value) relative to IR64 cultivar under nonlimiting conditions

G4: Temperature tolerance coefficient

(Adapted from Ahn et al., 2017)

Chapter 5.

RESULTS AND DISCUSSIONS

5.1. Technical Validation

5.1.1. Hydrologic Model Validation

The VIC has many parameters based on satellite-based observations, thus it is essential to adjust some of the parameters for reducing the differences in observed and simulated output. The VIC has been calibrated for a large number of applications at regional and global scale (Crow et al., 2003; Sheffield and Wood., 2007), so no calibration was performed for this study. Instead the VIC was validated against SMAP (Soil Moisture Active Passive) soil moisture for two years at a grid resolution of 36 km. Figure 12. illustrates the validation of annual mean soil moisture for 2017, showing good agreement with the observed surface soil moisture ($r = 0.8$). Figure 13. shows the correlation between SMAP soil moisture and model simulated soil moisture over Cambodia for 2016 and 2017, indicating a consistently high correlation seen in the eastern provinces. Except for some locations on the south and Tonle Sap Lake (showing low correlation), the VIC performs well with the SMAP observations over most areas. The SMAP soil moisture is independent of the model simulations, making it a suitable parameter for validation of the hydrologic model. Validation of soil moisture also provides confidence to the model performance, as the validated parameters are critical in characterizing the drought indices and basic hydrology of the region. Due to lack of continuous streamflow data in the region, the validation was only performed for soil moisture. For future works, the validation of VIC against streamflow and ET will be carried to further improve the model performance.

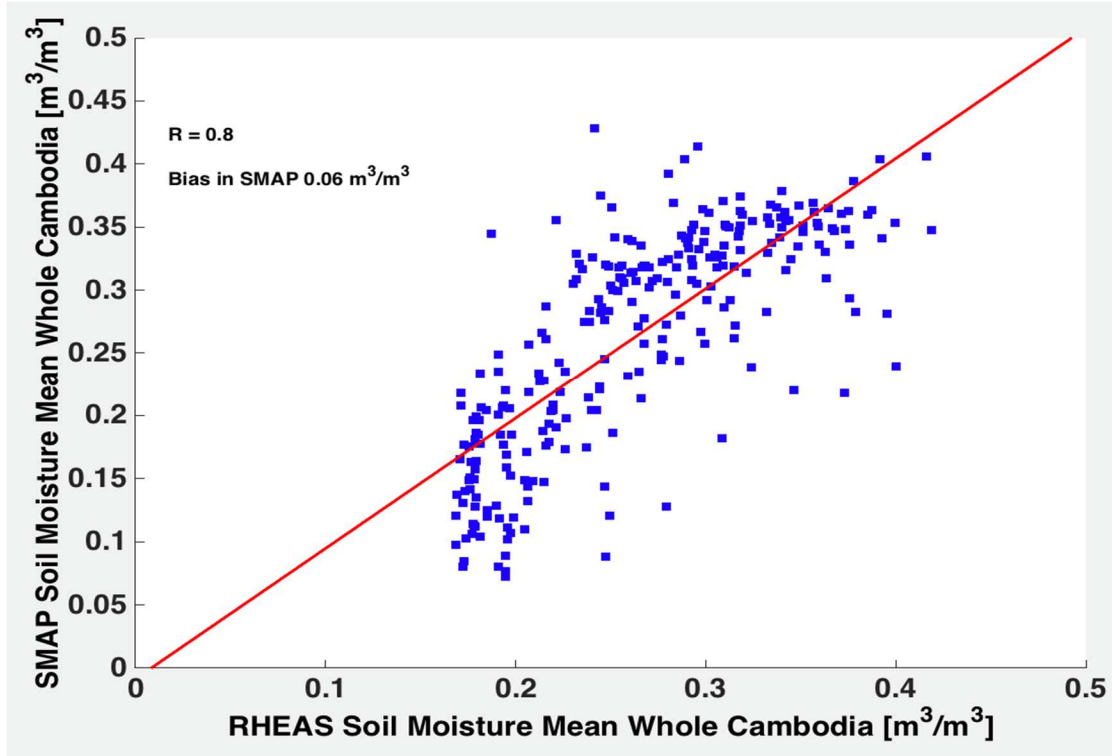


Figure 12. Comparison between RHEAS based surface soil moisture for 2017 data when compared with the SMAP surface soil moisture data (L3_SM_P) at 36 km EASE2 grid resolution

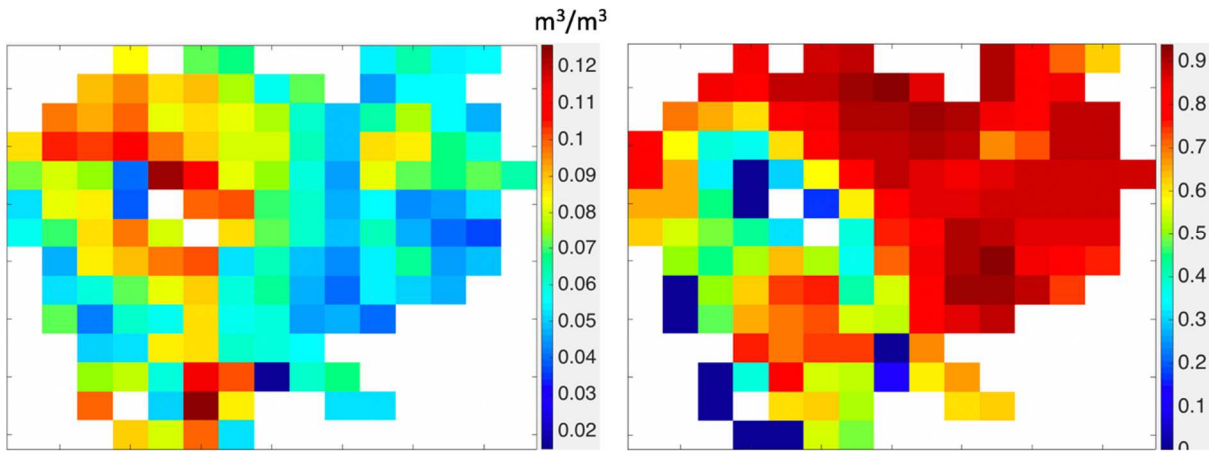


Figure 13. Unbiased RMSE: RHEAS based surface soil moisture for 2016 and 2017 data when compared with the SMAP surface soil moisture data (L3_SM_P) at 36 km EASE2 grid resolution (left); Correlation: RHEAS based surface soil moisture for 2016 and 2017 data when compared with the SMAP surface soil moisture data (L3_SM_P) at 36 km EASE2 grid resolution (right)

5.1.2. Crop Model Validation

Evaluation of crop productivity using crop models under various crop management practices is highly dependent on the calibration and validation of different parameters. The DSSAT Rice model validation is based on comparing the end-of-season simulated and observed yield. Although DSSAT contains many parameters, it is appropriate to adjust some parameters during calibration. The Genetic Coefficients, Fertilizer Application Rates are some of the common parameters adjusted during the calibration of DSSAT. The genetic coefficient for both cultivars was estimated using the GENCALC program in DSSAT (Table 5). The actual food and agriculture data were obtained from FAOSTAT (<http://www.fao.org/faostat/en/#data/QC>). Figure 14. shows a comparison of observed vs. simulated rice yields in Cambodia from 2000-2016. The model performed well ($R^2 = 0.83$) in capturing the observed trend at the middle of the simulation period (2008 onwards) as compared to the earlier years. The large difference of actual yield with model output during the initial simulation years (2000-2007) can be attributed to the mismatch of cultivar varieties, fertilizer rates, and other management practices during the initial years, thus making it difficult to capture observed trend. However, with gradual availability of information about the management practices, improvement in pesticide applications and use of genetically advanced rice varieties, the trend between observed and simulated yield show good agreement. Figure 15. shows a comparison between observed and simulated yield over Cambodia from 2008-2016, showing excellent trend with the observed data. In other words, the RHEAS performed well from 2008 onwards but on average were slightly higher than the actual yields.

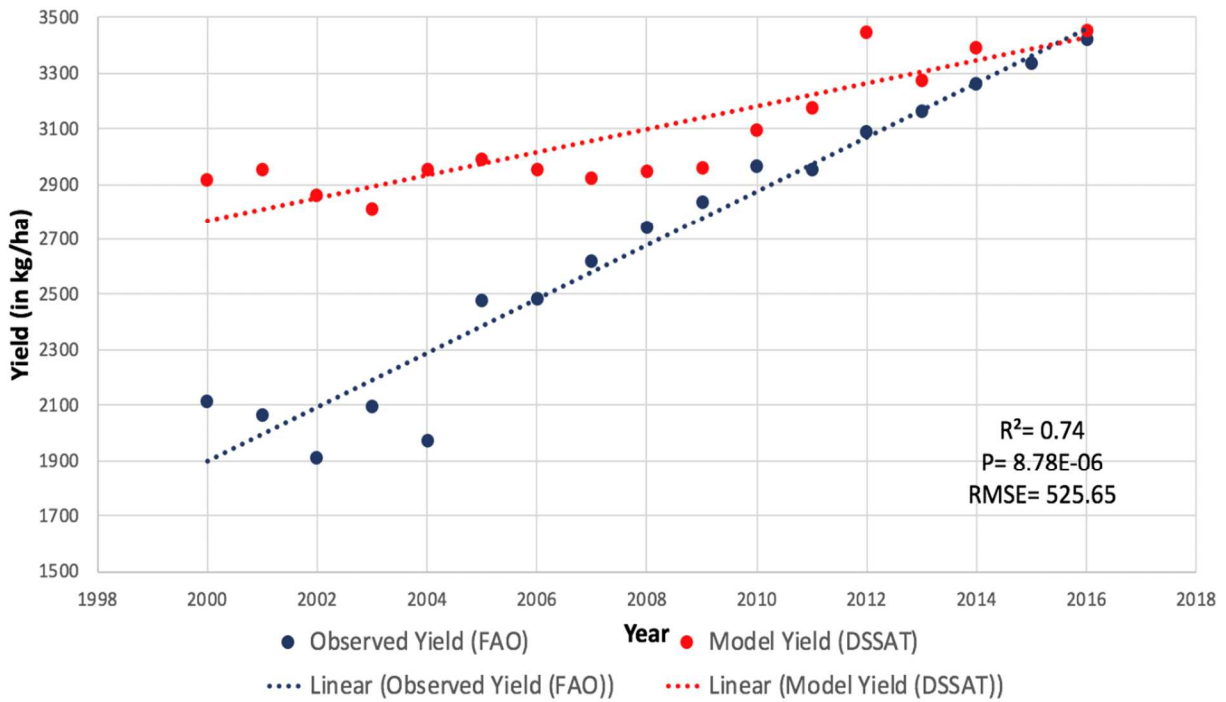


Figure 14. Comparison of actual yield records from FAO and RHEAS (DSSAT) simulations for rice in Cambodia from 2000-2016

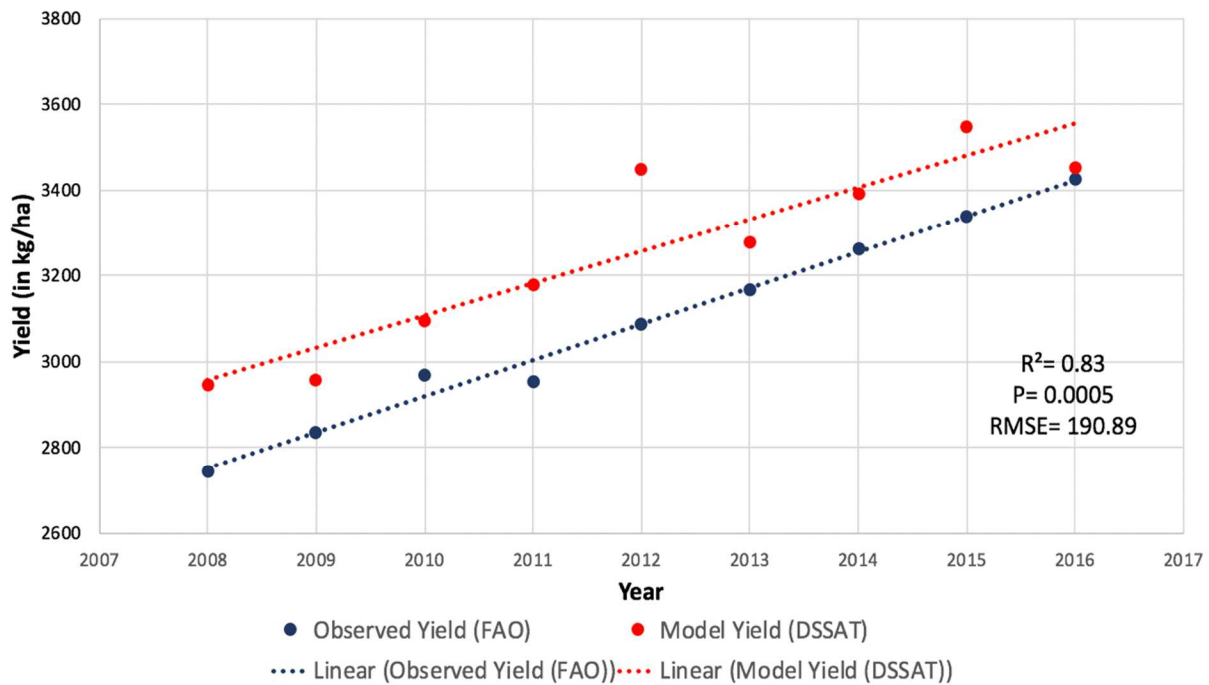


Figure 15. Best fit result between observed and model simulated rice yields from 2008-2016

5.2. Hydrologic Modeling: VIC

The implementation of RHEAS was performed over Cambodia to evaluate the hydrological and agricultural nowcasts for facilitating better decision making. The hydrologic model computes the land surface water balance for each grid cell on a daily basis over Cambodia. The final products of the hydrologic simulations produce a set of hydrologic and drought parameters for each grid cell. Final products (e.g. soil moisture, temperature, precipitation) derived from the hydrologic model that are directly related to water stress are given in both absolute values and anomalies. These variables are then used to construct the drought indicators such as the Standardized Precipitation Index, the Severity, and the Soil Moisture Deficit Index, among others. Based on the drought characteristics generated by the hydrologic model, the onset, duration and severity of drought can be understood. Figure 16. to Figure 20. presents the common drought monitoring outputs based on the RHEAS indicators. Figure 16. provides information about the 3-month standardized precipitation index over Cambodia, which is used to monitor meteorological drought. The 3-month SPI for Feb-Mar-Apr and Jun-Jul-Aug 2015 shows a good comparison between two dryness conditions over Cambodia. The initial period (Feb-Mar-Apr) of the year shows a moderate to severe dryness over the entire study area, while the second period (Jun-Jul-Aug) with the onset of southwest monsoon presents a near normal to moderate wet conditions. In other words, the 3-month SPI provides a comparison of the precipitation total over the 3-month period (Feb-Mar-Apr and Jun-Jul-Aug) in 2015 with precipitation totals for the same 3-months duration from the historical record (1987-2016). The 3-month SPI is useful to capture precipitation trends over Cambodia during reproductive and early grain-filling stages. Figure 16. also depicts the regional prevalence of severe drought conditions across the southeast provinces of Takeo and Prey Veng, with normal to moderate dryness conditions over the western provinces of Battambang and Pailin.

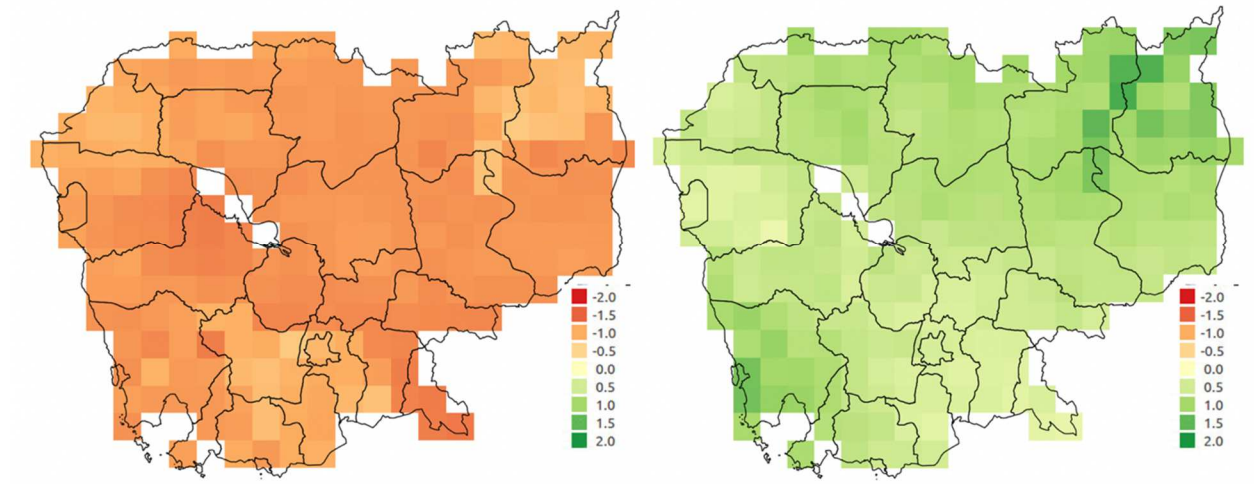


Figure 16. 3-month Standardized Precipitation Index over Cambodia for Feb-Mar-Apr (left), and Jun-Jul-Aug (right)

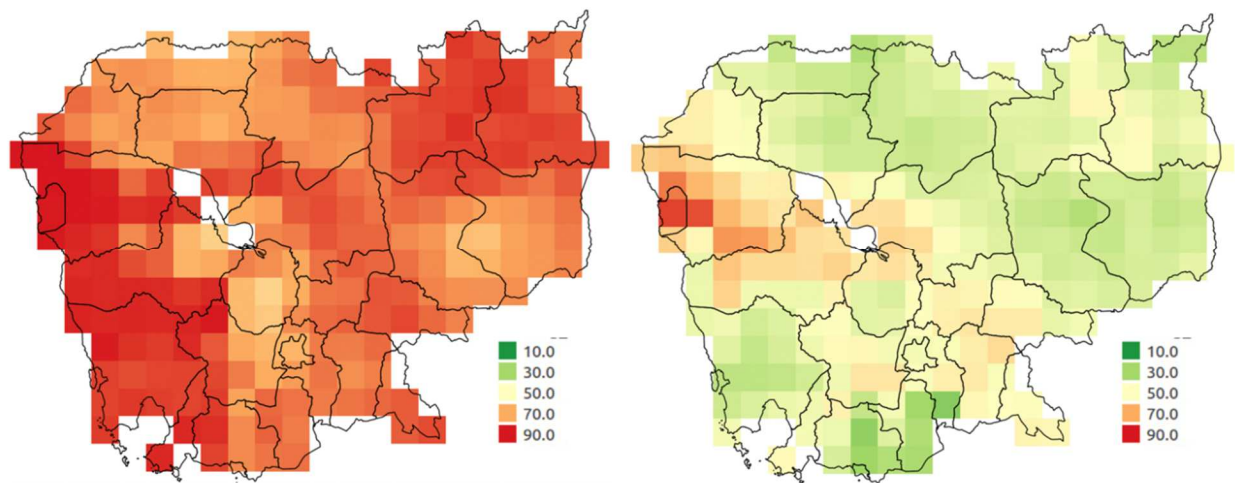


Figure 17. Agricultural drought severity over Cambodia for Mar-Apr-May (left), and Jun-Jul-Aug (right)

The 3-month SPI provides a better seasonal estimation of precipitation and short-to-medium term soil moisture conditions than the PDSI. The severity of drought gives an idea about the spatial intensity of drought over time. Figure 17. shows the spatial variation of the severity (intensity) of drought over Cambodia for period of Mar-Apr-May and Jun-Jul-Aug. From Figure 17., it can be clearly seen the drought severity more intense during the initial months (Mar-Apr-May) as

compared to the mid-months (Jun-Jul-Aug). The soil moisture deficit index was used to quantify agricultural drought using the weekly soil moisture values. Figure 18. presents the spatial distribution of soil moisture deficit index (SMDI) during the 22nd and 33rd week of 2015. SMDI shows good agreement with the spatial deficit of soil moisture when compared to drought severity (Figure 17.). The SMDI derived from the last week of May (22nd week) has more soil moisture deficit compared to the third-week of August (33rd week). Similar to the drought severity, the soil moisture deficit is more observed in the southwest and western provinces of Cambodia.

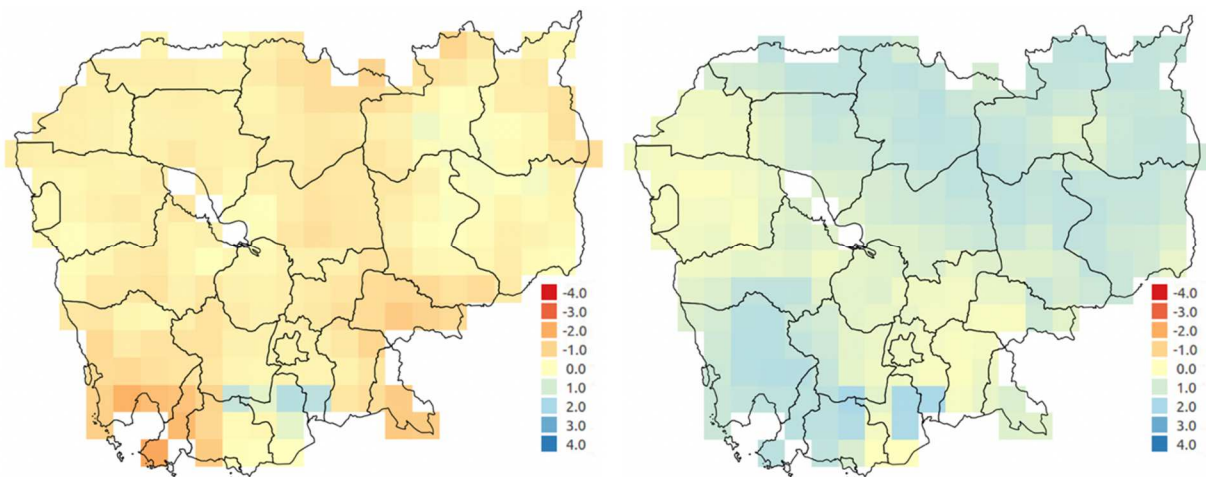


Figure 18. Spatial Distribution of Soil Moisture Deficit Index (SMDI) over Cambodia in 22nd week (last week of May) of 2015 (left), and 33rd week of 2015 (third week of August) (right)

Figure 19 and Figure 20 represents the accumulated precipitation and dryspells over Cambodia for the period of Mar-Apr-May and Jul-Aug-Sep (Aug-Sep-Oct for dryspells) in 2015. The annual precipitation totals during the initial period showed deficit in almost all provinces of the northwestern and southeastern portion of Cambodia, show a good correlation with SPI in capturing the deficits.

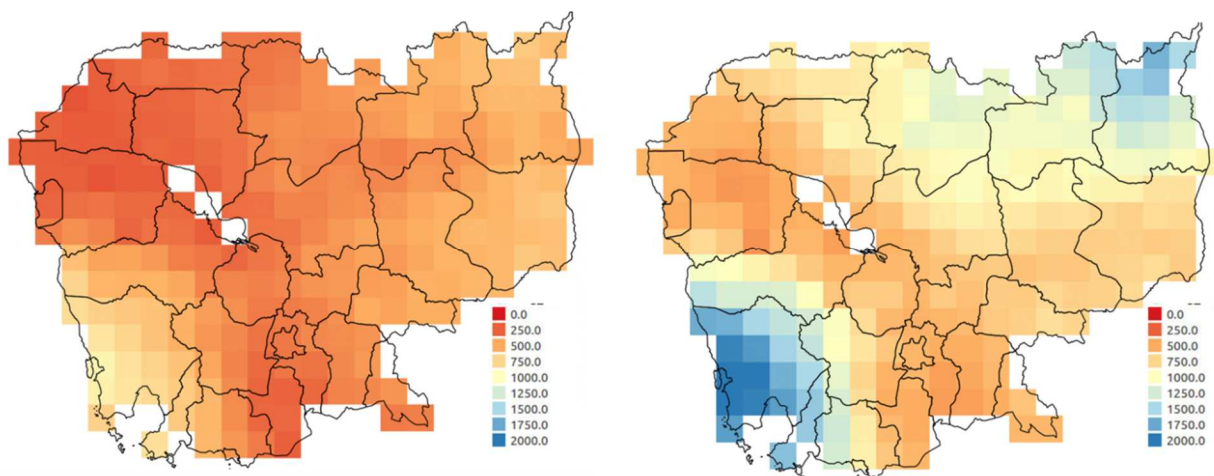


Figure 19. Annual Precipitation over Cambodia in 2015 for Mar-Apr-May (left), and Jul-Aug-Sep (right)

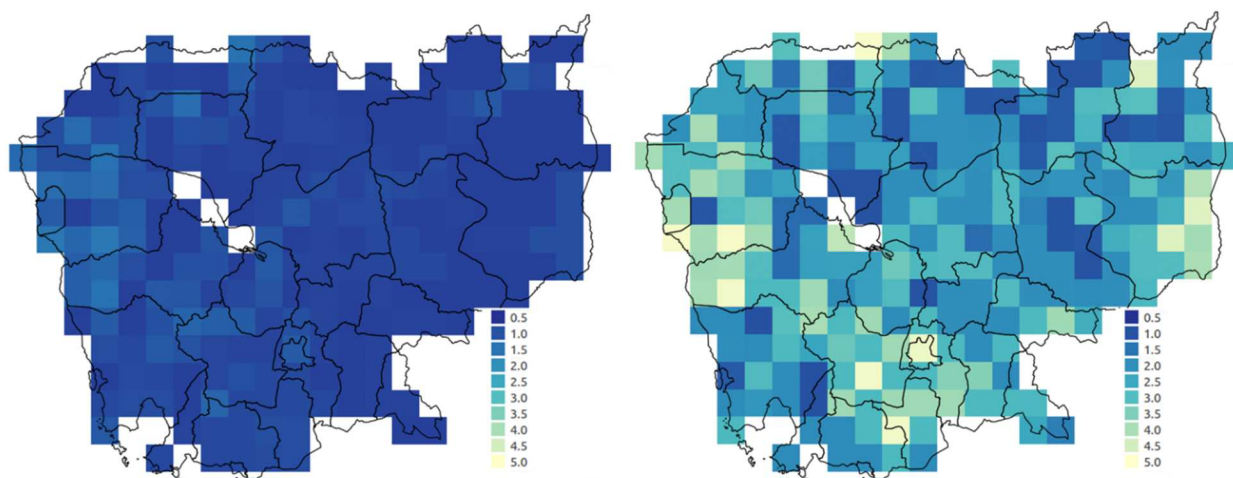


Figure 20. Dryspells period over Cambodia for Mar-Apr-May (left), and Aug-Sep-Oct (right)

Figure 21. illustrates the mean annual precipitation from 2000 to 2016, as obtained from RHEAS meteorological forcing. The precipitation amount has increased every year, with minimum rainfall totals in 2015 due to the prevalence of drought. The SPI, precipitation results from the forcing of gridded meteorological data to the RHEAS system, while indices like SMDI, soil moisture are simulated for each grid cells by the hydrologic model.

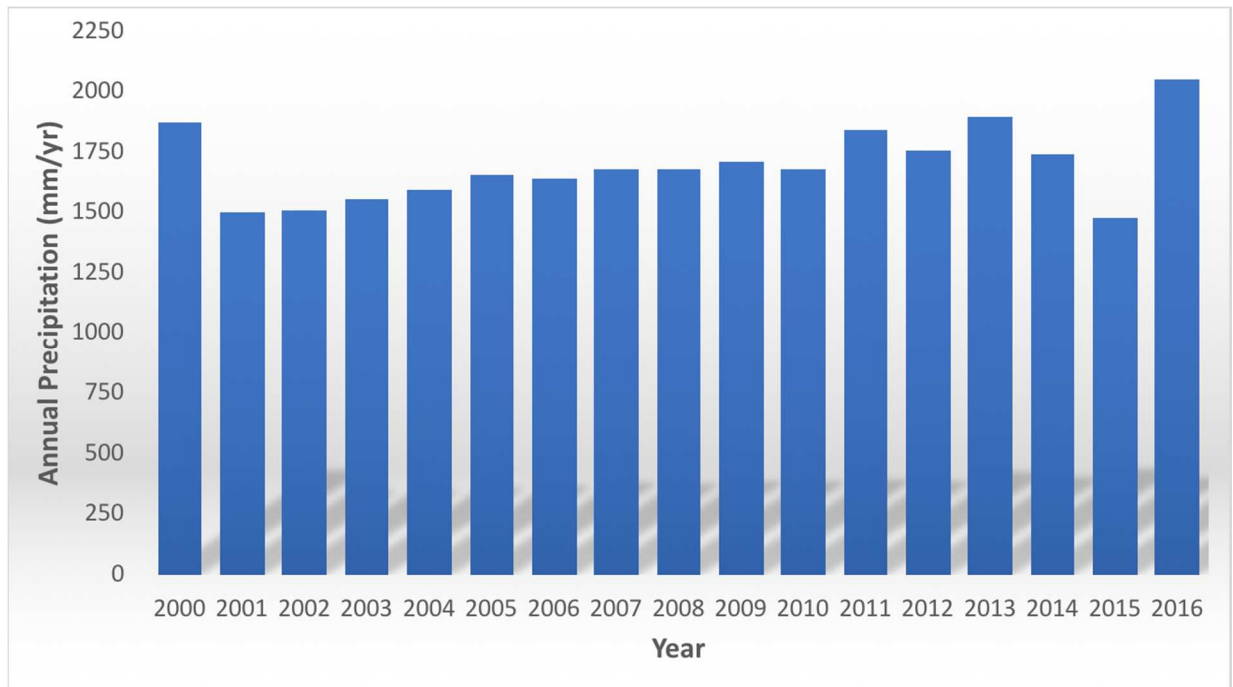


Figure 21. Annual precipitation (mm/year) time series over Cambodia from 2000-2016

5.3. Crop Modeling: DSSAT

One of the main goals of the study was to estimate the crop productivity in Lower Mekong (Cambodia) that could eventually be used by policy makers and growers to reduce the agricultural damages from drought. Figure 22. shows the simulated rice yield from RHEAS (DSSAT) over Cambodia in 2005 and 2015. The map clearly depicts the southeast provinces having the lowest yields in both stages, i.e. almost identical patterns of low yield is observed over the course of 10 years in those provinces, thus indicating the frequent exposure of the area to prolonged dry periods.

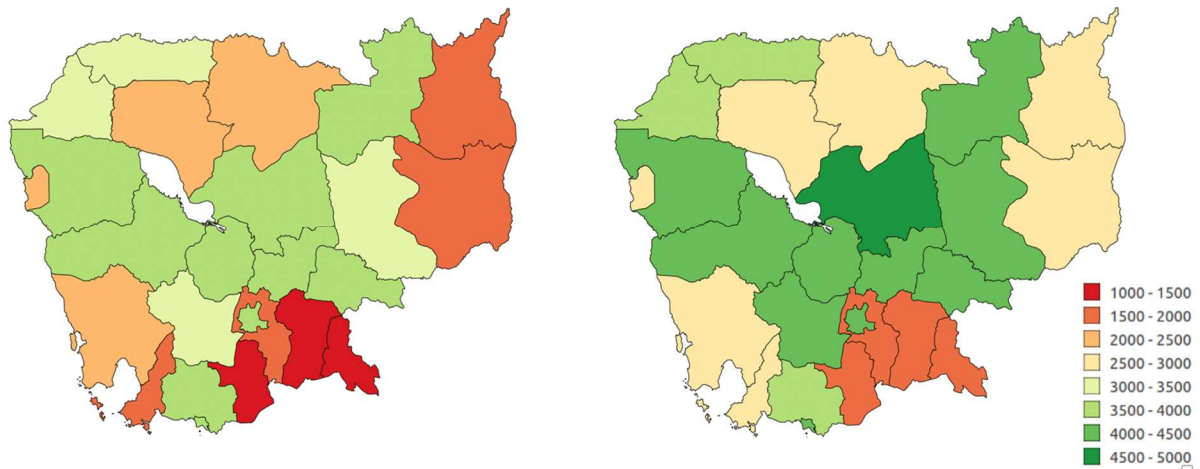


Figure 22. RHEAS (DSSAT) Output: Map of rice yield over Cambodia in 2005 (left) and 2015 (right) disaggregated to province level

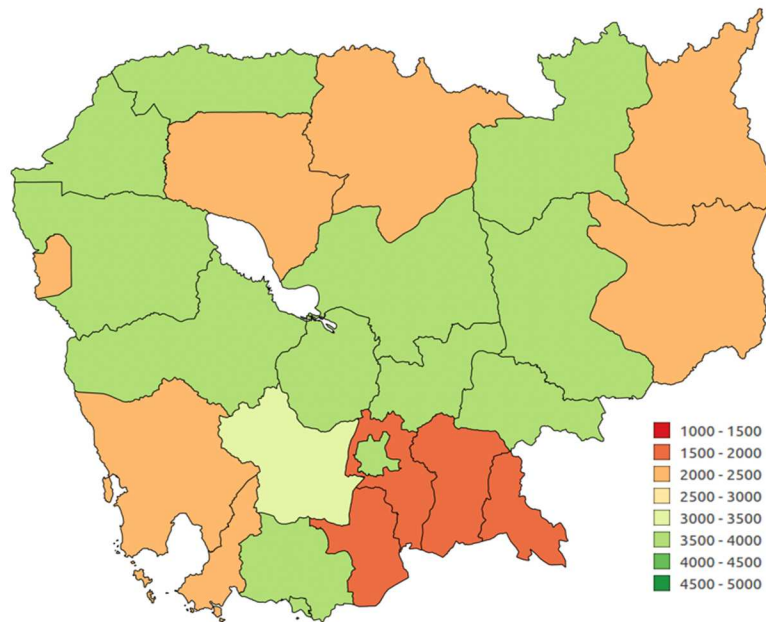


Figure 23. Rice Yields for each province of Cambodia from 2000-2016

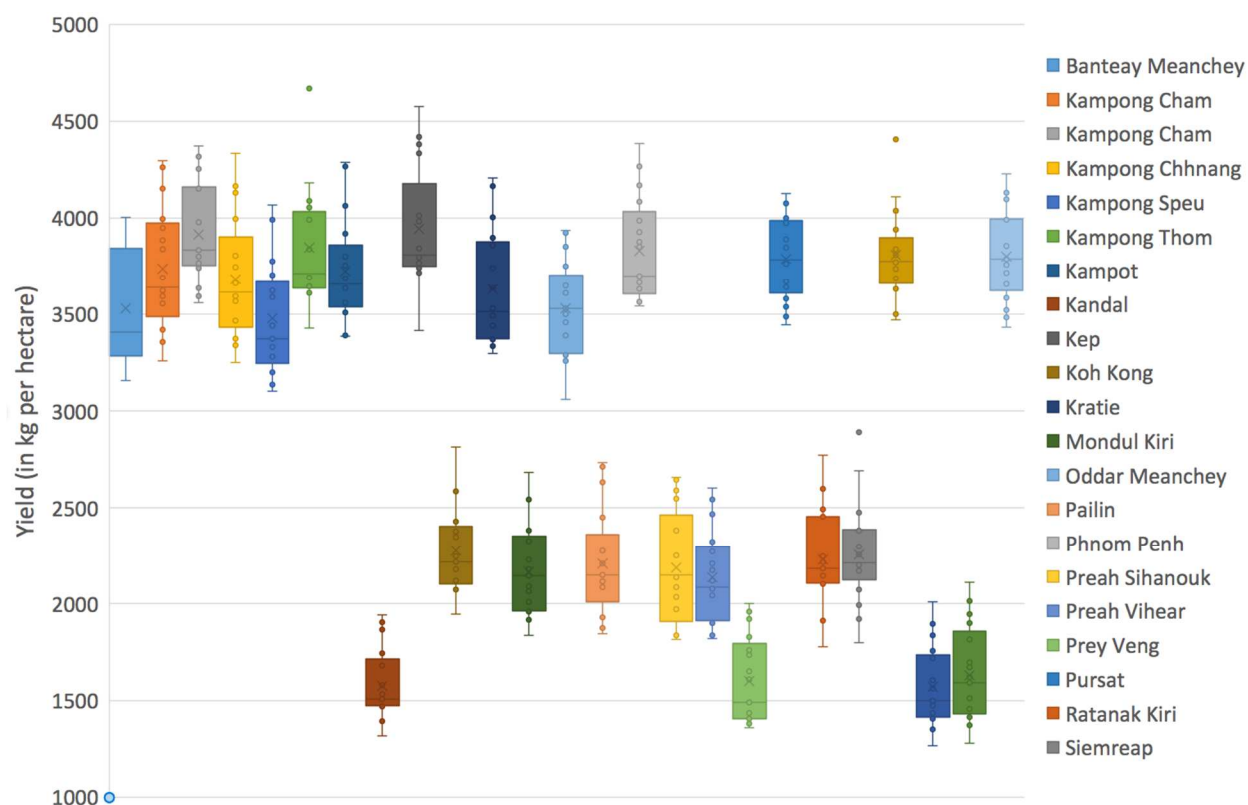


Figure 24. Provincial Rice yields over Cambodia from 2000-2016

But other areas, especially around the Tonle Sap basin, has seen increase in yield over time. According to the yield estimates of both the years, there has been an increase in average yield from 2005 to 2015, mainly due to technology and improvement in management practices. The average rice yields varied from 2900 kg/ha in 2005 to 3550 kg/ha 2015, mainly due to the use of high-yield cultivars and use of fertilizers and pesticides. The southeast provinces comprising of Kandal, Takeo, Prey Vang and Svay Rieng showed low yields due to its high vulnerability to drought events. The low yield can be attributed to the non-availability of water in some provinces due to lack of precipitation. The low crop productivity in the four provinces can also be well matched with the drought characteristics such as SPI and SMDI (Figure 16 and 18), where the southeastern provinces are areas with lowest yield due to exposure of large periods of dryness. Some areas like the western portion (Battambang) of Cambodia show high yield despite high drought severity.

This may be due to the soil properties and the adaptability of the crops to the local conditions. The Figure 24. shows the average rice yield over each province of Cambodia from 2000-2016, which indicates southeastern provinces having the lowest yields over the period of 16 years (Figure 23).

5.4. Technical Analyses: Impact of Drought on Rice Yields

In this section, we discuss the impact of drought on the rice yields over Cambodia for a period of 16 years. There are few drought indicators that are capable of capturing the interannual climate anomalies due to rainfall and temperature that ultimately influence the rice yield in a rainfed system. Prominent among these drought indicators is the 3-month SPI (i.e., SPI3). Therefore, we used this indicator to evaluate the rice yield across 16 years. The correlation between SPI3 and rice yields over each province of Cambodia were evaluated to study the impact of drought status on the rice yields. Figure 25 shows the correlation between SPI3 and crop yield over each Cambodian province. For a better understanding, the correlations between SPI3 and rice yields for a high yield and low yield province were analyzed (Figure 26), which depicted reasonable correlation with drought indicator. Intuitively, positive correlations between rice yields and SPI3 values were expected because for average and above average rainfall years mostly normal yields and above normal yields were found. However, SPI3 values did not explain all the variance in the rice yields across all the years. It was observed that provinces showing a negative correlation with SPI3 values were the same provinces having consistently low yields between 2000-2016. Low and negative correlations observed in the eleven provinces were attributed to the soil type and persistent low SPI3. During the study period, for the whole country (Cambodia), the actual yields show an increasing trend that is attributed to the increased application of fertilizer (nitrogen-based) and country-wide normal or above normal rainfall. Further analyses quantifying the impacts of

drought on rice yield is planned for future works that will involve crop modeling since 1981 to obtain more robust statistics and evidence.

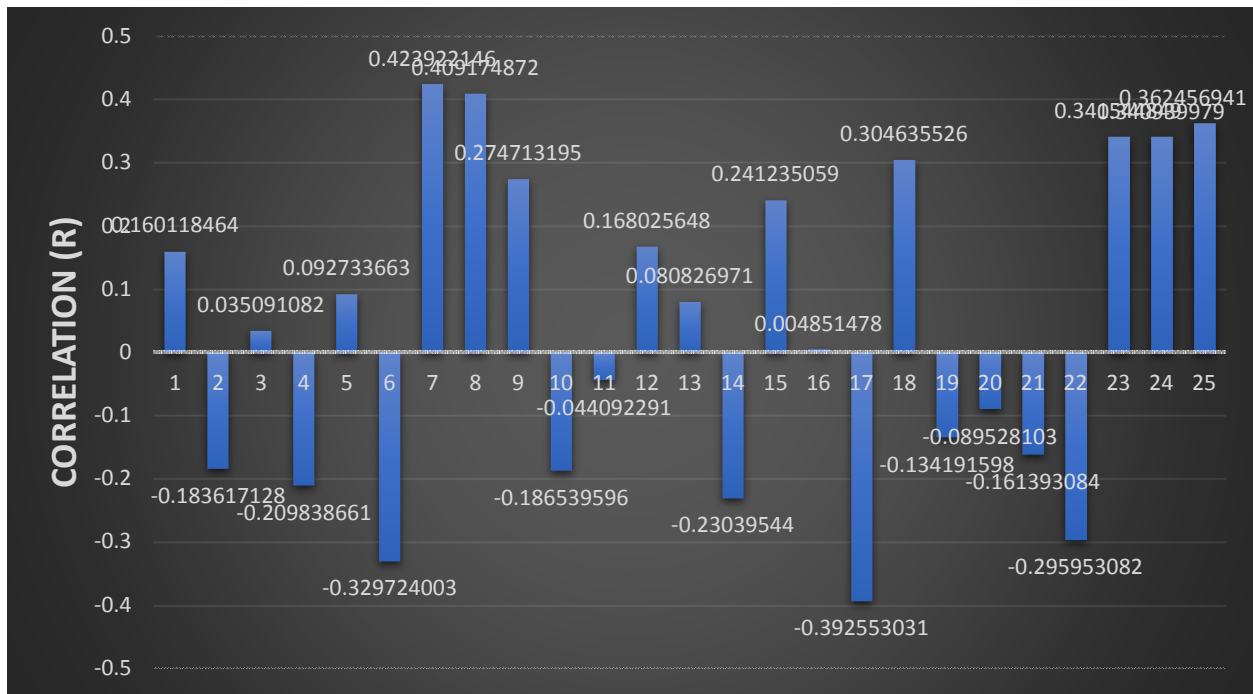


Figure 25. Correlation between 3-month SPI and rice yield over all provinces of Cambodia for J-J-A, 2000-2016

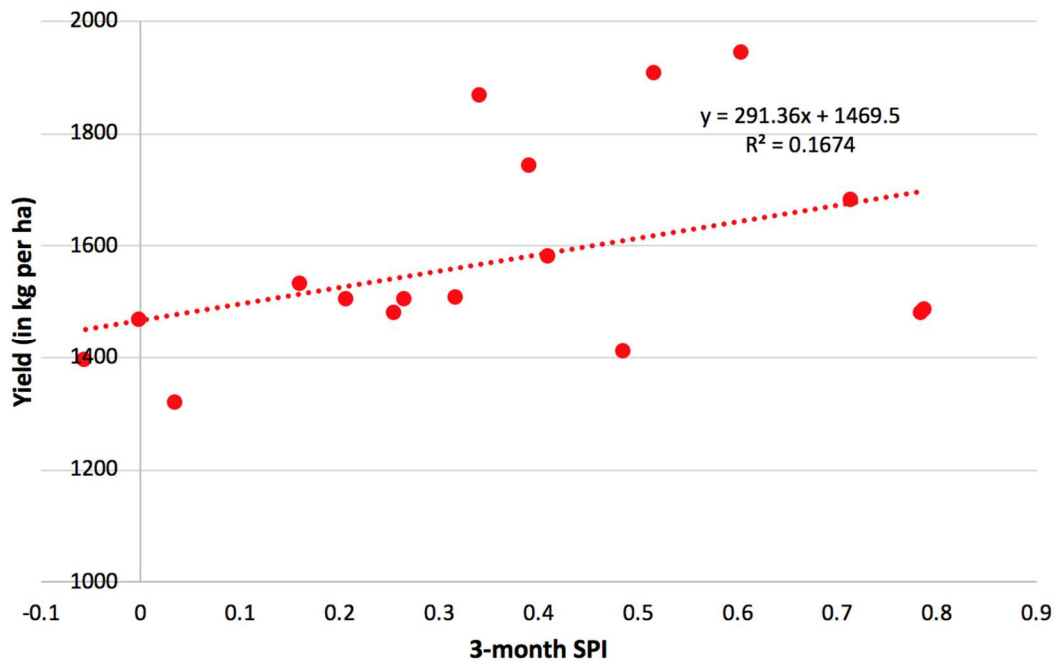
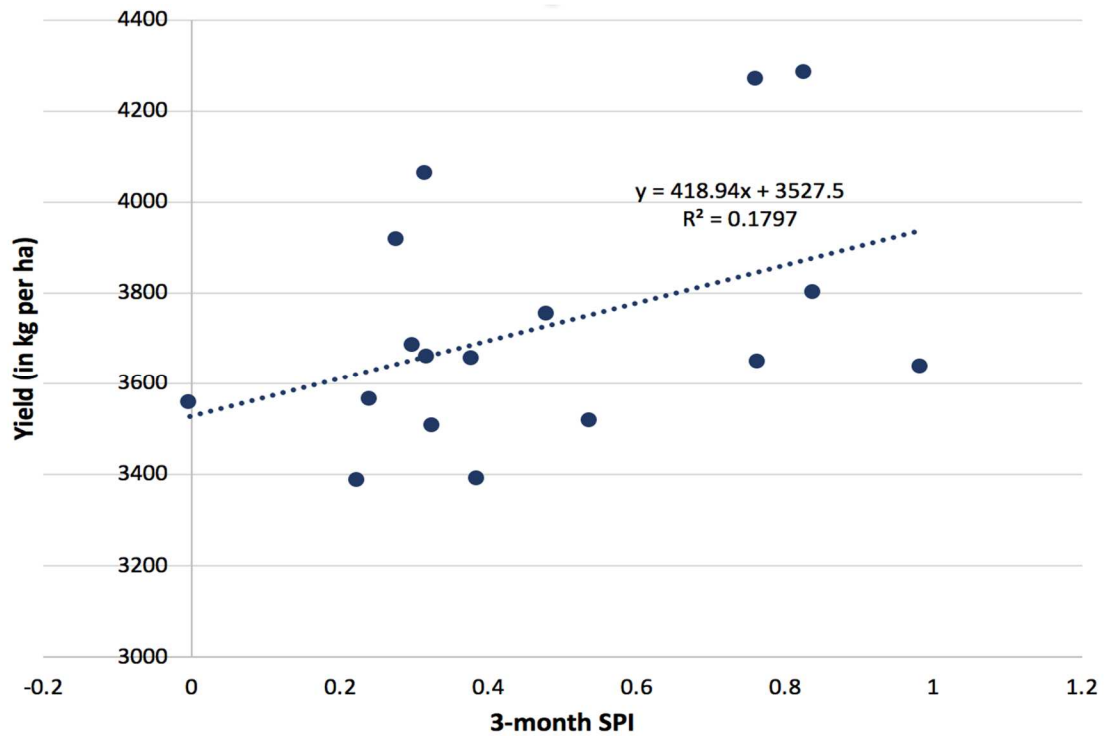


Figure 26. Correlation between 3-month SPI and rice yield for J-J-A from 2000-16 over Kampot (top), and Kandal (bottom) province of Cambodia

Chapter 6.

CONCLUSION

The proposed hydrologic framework- RHEAS, presented in the study showcased the potential of the model for effective drought and crop monitoring, thus demonstrating its readiness for seasonal probabilistic forecasts over the Lower Mekong region. RHEAS performed well in capturing the meteorological and agricultural drought over Cambodia based on SPI, SMDI, severity. For 2015, the model analyzed severe drought conditions over the entire country for the initial months, but gradually with the onset of monsoon at the beginning of growing season there was no significant prevalence of drought conditions. In other words, moderate to severe drought were concentrated from Feb - May, with near-normal to moderate wet conditions during the growing season. Changes in soil moisture and precipitation were observed with occurrence of precipitation anomalies. The study also demonstrated the relationship between drought and crop yield, with the southeastern provinces showing low yields as a result of frequent exposure to dry periods from 2000-2016. Results from this study, especially the drought indicators and crop yields were validated against real-time data for evaluating the performance of model. The simulated soil moisture exhibited a high correlation ($r = 0.8$), when validated with SMAP surface soil moisture. The validation of RHEAS simulations of yields in response to drought with actual yield estimates presented a good correlation from 2008-2016 by capturing the inter-annual variability. The magnitude of yield gap between actual and model estimates during the earlier simulation years was due to the use of same variety of rice for the entire study period, whereas in reality the cultivar variety and management practices (fertilizer rates) were different during 2000-2007. The study strongly inferred the use of nitrogenous fertilizers as the major factor for achieving such high yields. Due to the unavailability of information about provincial yields, the crop model validation was done using the actual yield

data from FAO for the entire country. The results from RHEAS over Cambodia marks an important step towards making an operational drought and crop yield forecasting system in the Lower Mekong Basin countries for better decision making.

To reduce the effects of drought on agriculture, the use of monitoring systems is not sufficient for capturing the subtle growth of drought over time. RHEAS targets to provide probabilistic seasonal forecasts by using the historical drought severity data and nowcast simulations, which will be helpful in taking preventive measures against drought onset over the Lower Mekong Basin. For improving the performance of the model, the technical validation approaches also need to be improved. Currently, RHEAS plan to validate the hydrologic model against ET, in addition to the soil moisture data. With the availability of continuous streamflow data from the local *in-situ* stations, RHEAS can also be validated against streamflow in future, thus providing more confidence to the model performance. Special attention is also required to make the findings available on a regular basis and providing drought and crop yield forecasts to the local bodies and government agencies for better planning and risk management against drought. As RHEAS is a relatively new hydrologic framework, there are many uncertainties about the performance and applications in real scenarios as compared to the existing developed hydrologic and crop models, but with the initial real-time application over Cambodia, the model performance is anticipated to improve over time.

BIBLIOGRAPHY

BIBLIOGRAPHY

Ahn, J., 2017. Shifting Planting Dates and Fertilizer Application Rates as Climate Change Adaptation Strategies for Two Rice Cultivars in Cambodia. *한국기후변화학회지*, 8(3), pp.187-199.

Allen, C.D., Macalady, A.K., Chenchouni, H., Bachelet, D., McDowell, N., Vennetier, M., Kitzberger, T., Rigling, A., Breshears, D.D., Hogg, E.T. and Gonzalez, P., 2010. A global overview of drought and heat-induced tree mortality reveals emerging climate change risks for forests. *Forest ecology and management*, 259(4), pp.660-684.

Andreadis, K.M., Clark, E.A., Wood, A.W., Hamlet, A.F. and Lettenmaier, D.P., 2005. Twentieth-century drought in the conterminous United States. *Journal of Hydrometeorology*, 6(6), pp.985-1001.

Andreadis, K.M., Das, N., Stampoulis, D., Ines, A., Fisher, J.B., Granger, S., Kawata, J., Han, E. and Behrangi, A., 2017. The Regional Hydrologic Extremes Assessment System: A software framework for hydrologic modeling and data assimilation. *PloS one*, 12(5), p.e0176506.

Andreadis, K.M., Storck, P. and Lettenmaier, D.P., 2009. Modeling snow accumulation and ablation processes in forested environments. *Water Resources Research*, 45(5).

Annual Disaster Statistical Review 2016, Centre for Research on the Epidemiology of Disasters (CRED)

Arrouays, D., Grundy, M.G., Hartemink, A.E., Hempel, J.W., Heuvelink, G.B., Hong, S.Y., Lagacherie, P., Lelyk, G., McBratney, A.B., McKenzie, N.J. and dL Mendonca-Santos, M., 2014. GlobalSoilMap: Toward a fine-resolution global grid of soil properties. In *Advances in agronomy* (Vol. 125, pp. 93-134). Academic Press.

Asian Disaster Preparedness Centre, 2002

Barros, V.R., Field, C.B., Dokke, D.J., Mastrandrea, M.D., Mach, K.J., Bilir, T.E., Chatterjee, M., Ebi, K.L., Estrada, Y.O., Genova, R.C. and Girma, B., 2014. Climate change 2014: impacts, adaptation, and vulnerability-Part B: regional aspects-Contribution of Working Group II to the Fifth Assessment Report of the Intergovernmental Panel on Climate Change.

Bowling, L.C. and Lettenmaier, D.P., 2010. Modeling the effects of lakes and wetlands on the water balance of Arctic environments. *Journal of Hydrometeorology*, 11(2), pp.276-295.

Brown, A.E., Zhang, L., McMahon, T.A., Western, A.W. and Vertessy, R.A., 2005. A review of paired catchment studies for determining changes in water yield resulting from alterations in vegetation. *Journal of hydrology*, 310(1-4), pp.28-61.

Bruijnzeel, L.A., 2004. Hydrological functions of tropical forests: not seeing the soil for the trees?. *Agriculture, ecosystems & environment*, 104(1), pp.185-228.

Carrao, H., Naumann, G. and Barbosa, P., 2016. Mapping global patterns of drought risk: An empirical framework based on sub-national estimates of hazard, exposure and vulnerability. *Global Environmental Change*, 39, pp.108-124.

Cherkauer, K.A., Bowling, L.C. and Lettenmaier, D.P., 2003. Variable infiltration capacity cold land process model updates. *Global and Planetary Change*, 38(1-2), pp.151-159.

Cutler, P. and Stephenson, R., 1984. *The state of food emergency preparedness in Ethiopia*. Relief and Development Institute (International Disaster Institute).

Dai, A., 2013. Increasing drought under global warming in observations and models. *Nature Climate Change*, 3(1), p.52.

Dai, A., Trenberth, K.E. and Qian, T., 2004. A global dataset of Palmer Drought Severity Index for 1870–2002: Relationship with soil moisture and effects of surface warming. *Journal of Hydrometeorology*, 5(6), pp.1117-1130.

Economic Outlook for Southeast Asia, China and India, 2018

Edwards, D.C., 1997. *Characteristics of 20th century drought in the United States at multiple time scales* (No. AFIT-97-051). AIR FORCE INST OF TECH WRIGHT-PATTERSON AFB OH.

Funk, C., Peterson, P., Landsfeld, M., Pedreros, D., Verdin, J., Shukla, S., Husak, G., Rowland, J., Harrison, L., Hoell, A. and Michaelsen, J., 2015. The climate hazards infrared precipitation with stations—a new environmental record for monitoring extremes. *Scientific data*, 2, p.150066.

Global Energy and CO2 status Report, International Energy Agency, 2017

Godfray, H.C.J., Beddington, J.R., Crute, I.R., Haddad, L., Lawrence, D., Muir, J.F., Pretty, J., Robinson, S., Thomas, S.M. and Toulmin, C., 2010. Food security: the challenge of feeding 9 billion people. *science*, 327(5967), pp.812-818.

Grasso, V.F. and Singh, A., 2011. Early warning systems: State-of-art analysis and future directions. *Draft report, UNEP*, 1.

Gu, Y., Brown, J.F., Verdin, J.P. and Wardlow, B., 2007. A five-year analysis of MODIS NDVI and NDWI for grassland drought assessment over the central Great Plains of the United States. *Geophysical Research Letters*, 34(6).

Guha-Sapir, D., Vos, F., Below, R. and Ponsérre, S., 2012. *Annual disaster statistical review 2011: the numbers and trends*. Centre for Research on the Epidemiology of Disasters (CRED).

Hao, Z. and AghaKouchak, A., 2014. A nonparametric multivariate multi-index drought monitoring framework. *Journal of Hydrometeorology*, 15(1), pp.89-101.

Hao, Z., Yuan, X., Xia, Y., Hao, F. and Singh, V.P., 2017. An overview of drought monitoring and prediction systems at regional and global scales. *Bulletin of the American Meteorological Society*, 98(9), pp.1879-1896.

Hayes, M., Svoboda, M., Wall, N. and Widhalm, M., 2011. The Lincoln declaration on drought indices: universal meteorological drought index recommended. *Bulletin of the American Meteorological Society*, 92(4), pp.485-488.

Hengl, T., de Jesus, J.M., MacMillan, R.A., Batjes, N.H., Heuvelink, G.B., Ribeiro, E., Samuel-Rosa, A., Kempen, B., Leenaars, J.G., Walsh, M.G. and Gonzalez, M.R., 2014. SoilGrids1km—global soil information based on automated mapping. *PloS one*, 9(8), p.e105992.

Hundertmark, W., 2008. Building drought management capacity in the Mekong River basin. *Irrigation and Drainage: The journal of the International Commission on Irrigation and Drainage*, 57(3), pp.279-287.

Ines, A.V., Das, N.N., Hansen, J.W. and Njoku, E.G., 2013. Assimilation of remotely sensed soil moisture and vegetation with a crop simulation model for maize yield prediction. *Remote Sensing of Environment*, 138, pp.149-164.

IWRM (2011)-Based Basin Development Strategy for the Lower Mekong Basin (Mekong River Commission, Vientiane, Lao PDR).

Jansson, P., Hock, R. and Schneider, T., 2003. The concept of glacier storage: a review. *Journal of Hydrology*, 282(1-4), pp.116-129.

Jones, J.W., Hoogenboom, G., Porter, C.H., Boote, K.J., Batchelor, W.D., Hunt, L.A., Wilkens, P.W., Singh, U., Gijsman, A.J. and Ritchie, J.T., 2003. The DSSAT cropping system model. *European journal of agronomy*, 18(3-4), pp.235-265.

Kalnay, E., Kanamitsu, M., Kistler, R., Collins, W., Deaven, D., Gandin, L., Iredell, M., Saha, S., White, G., Woollen, J. and Zhu, Y., 1996. The NCEP/NCAR 40-year reanalysis project. *Bulletin of the American meteorological Society*, 77(3), pp.437-472.

Kirby, M. and Mainuddin, M., 2009. Water and agricultural productivity in the Lower Mekong Basin: trends and future prospects. *Water International*, 34(1), pp.134-143.

Kite, G., 2001. Modelling the Mekong: hydrological simulation for environmental impact studies. *Journal of Hydrology*, 253(1-4), pp.1-13.

Kumar, B.G., 1990. Ethiopian famines 1973–1985: A case-study. *The political economy of hunger*, 2, pp.173-216.

Liang, X., Lettenmaier, D.P. and Wood, E.F., 1996. One-dimensional statistical dynamic representation of subgrid spatial variability of precipitation in the two-layer variable infiltration capacity model. *Journal of Geophysical Research: Atmospheres*, 101(D16), pp.21403-21422.

Liang, X., Lettenmaier, D.P., Wood, E.F. and Burges, S.J., 1994. A simple hydrologically based model of land surface water and energy fluxes for general circulation models. *Journal of Geophysical Research: Atmospheres*, 99(D7), pp.14415-14428.

Liu, Shaochuang & Lu, P & Liu, D & Jin, P & Wang, W. (2009). Pinpointing the sources and measuring the lengths of the principal rivers of the world. *Int. J. Digital Earth*. 2. 80-87. 10.1080/17538940902746082.

Lu, E., Luo, Y., Zhang, R., Wu, Q. and Liu, L., 2011. Regional atmospheric anomalies responsible for the 2009–2010 severe drought in China. *Journal of Geophysical Research: Atmospheres*, 116(D21).

Makokha, G.O., Wang, L., Zhou, J., Li, X., Wang, A., Wang, G. and Kuria, D., 2016. Quantitative drought monitoring in a typical cold river basin over Tibetan Plateau: An integration of meteorological, agricultural and hydrological droughts. *Journal of Hydrology*, 543, pp.782-795.

Meehl, G.A., Stocker, T.F., Collins, W.D., Friedlingstein, P., Gaye, T., Gregory, J.M., Kitoh, A., Knutti, R., Murphy, J.M., Noda, A. and Raper, S.C., 2007. Global climate projections.

Mehran, A., Mazdiyasni, O. and AghaKouchak, A., 2015. A hybrid framework for assessing socioeconomic drought: Linking climate variability, local resilience, and demand. *Journal of Geophysical Research: Atmospheres*, 120(15), pp.7520-7533.

Mekong River Commission, 2014

Mekong River Commission. *State of the Basin Report*. (Vientiane, Lao PDR), 232 pp (2010).

Ministry of Agriculture, Forestry and Fisheries, 2010

Ministry of Environment, 2001 (For Cambodia: refer Literature Review)

Mishra, A.K. and Singh, V.P., 2010. A review of drought concepts. *Journal of hydrology*, 391(1-2), pp.202-216.

MRC (2003) Social Atlas of the Lower Mekong Basin. Mekong River Commission

MRC (2009a) Agriculture sector information for the economic, environment and social assessment of the considered basin-wide development scenarios.

MRC (2009b) Multi-functionality of paddy fields over the Lower Mekong Basin. MRC Technical paper. November, 2009

MRC (2010a) Supporting Technical Notes. Assessment of Basin-wide Development Scenarios, Supporting Technical Notes.

MRC (2010b), Assessment of Basin-Wide Scenarios, Agricultural Impacts, Technical Note #7, Mekong River Commission, Vientiane, Lao PDR

Mu, Q., Zhao, M., Kimball, J.S., McDowell, N.G. and Running, S.W., 2013. A remotely sensed global terrestrial drought severity index. *Bulletin of the American Meteorological Society*, 94(1), pp.83-98.

Narasimhan, B. and Srinivasan, R., 2005. Development and evaluation of Soil Moisture Deficit Index (SMDI) and Evapotranspiration Deficit Index (ETDI) for agricultural drought monitoring. *Agricultural and Forest Meteorology*, 133(1-4), pp.69-88.

Nijssen, B., Shukla, S., Lin, C., Gao, H., Zhou, T., Sheffield, J., Wood, E.F. and Lettenmaier, D.P., 2014. A prototype global drought information system based on multiple land surface models. *Journal of Hydrometeorology*, 15(4), pp.1661-1676.

Ntale, H.K. and Gan, T.Y., 2003. Drought indices and their application to East Africa. *International Journal of Climatology*, 23(11), pp.1335-1357.

Obe, R. and Hsu, L., 2015. PostGIS in Action. Greenwich, CT.

Pokhrel, Y., Burbano, M., Roush, J., Kang, H., Sridhar, V. and Hyndman, D.W., 2018. A Review of the Integrated Effects of Changing Climate, Land Use, and Dams on Mekong River Hydrology. *Water*, 10(3), p.266.

Population 2030, Economic and Social Affairs, United Nations, 2015a

Porkka, M., Gerten, D., Schaphoff, S., Siebert, S. and Kummu, M., 2016. Causes and trends of water scarcity in food production. *Environmental Research Letters*, 11(1), p.015001.

REN21, R., 2017. Global Status Report, REN21 Secretariat, Paris, France. In *Tech. Rep.*.

Rhee, J., Im, J. and Carbone, G.J., 2010. Monitoring agricultural drought for arid and humid regions using multi-sensor remote sensing data. *Remote Sensing of Environment*, 114(12), pp.2875-2887.

Sawano, S., Hasegawa, T., Goto, S., Konghakote, P., Polthanee, A., Ishigooka, Y., Kuwagata, T. and Toritani, H., 2008. Modeling the dependence of the crop calendar for rain-fed rice on precipitation in Northeast Thailand. *Paddy and Water Environment*, 6(1), pp.83-90.

Sheffield, J. and Wood, E.F., 2007. Characteristics of global and regional drought, 1950–2000: Analysis of soil moisture data from off-line simulation of the terrestrial hydrologic cycle. *Journal of Geophysical Research: Atmospheres*, 112(D17).

- Sheffield, J., Goteti, G. and Wood, E.F., 2006. Development of a 50-year high-resolution global dataset of meteorological forcings for land surface modeling. *Journal of Climate*, 19(13), pp.3088-3111.
- Sheffield, J., Goteti, G., Wen, F. and Wood, E.F., 2004. A simulated soil moisture based drought analysis for the United States. *Journal of Geophysical Research: Atmospheres*, 109(D24).
- Sheffield, J., Wood, E.F. and Roderick, M.L., 2012. Little change in global drought over the past 60 years. *Nature*, 491(7424), p.435.
- Shukla, S., Sheffield, J., Wood, E.F. and Lettenmaier, D.P., 2013. On the sources of global land surface hydrologic predictability. *Hydrology & Earth System Sciences*, 17(7).
- Son, N.T., Chen, C.F., Chen, C.R., Chang, L.Y. and Minh, V.Q., 2012. Monitoring agricultural drought in the Lower Mekong Basin using MODIS NDVI and land surface temperature data. *International Journal of Applied Earth Observation and Geoinformation*, 18, pp.417-427.
- Sruthi, S. and Aslam, M.M., 2015. Agricultural drought analysis using the NDVI and land surface temperature data; a case study of Raichur district. *Aquatic Procedia*, 4, pp.1258-1264.
- Staudinger, M., Stahl, K. and Seibert, J., 2014. A drought index accounting for snow. *Water Resources Research*, 50(10), pp.7861-7872.
- Steduto, P., Hsiao, T.C., Raes, D. and Fereres, E., 2009. AquaCrop—The FAO crop model to simulate yield response to water: I. Concepts and underlying principles. *Agronomy Journal*, 101(3), pp.426-437.
- Steinemann, A.C. and Cavalcanti, L.F., 2006. Developing multiple indicators and triggers for drought plans. *Journal of Water Resources Planning and Management*, 132(3), pp.164-174.
- Sun, L., Mitchell, S.W. and Davidson, A., 2012. Multiple drought indices for agricultural drought risk assessment on the Canadian prairies. *International Journal of Climatology*, 32(11), pp.1628-1639.
- Svoboda, M., Hayes, M. and Wood, D., 2012. Standardized precipitation index user guide. *World Meteorological Organization Geneva, Switzerland*.
- Thirumalai, K., DiNezio, P.N., Okumura, Y. and Deser, C., 2017. Extreme temperatures in Southeast Asia caused by El Nino and worsened by global warming. *Nature communications*, 8, p.15531.
- Umran Komuscu, A., 1999. Using the SPI to analyze spatial and temporal patterns of drought in Turkey. *Drought Network News (1994-2001)*, p.49.
- Wang, L., Yuan, X., Xie, Z., Wu, P. and Li, Y., 2016. Increasing flash droughts over China during the recent global warming hiatus. *Scientific Reports*, 6, p.30571.

Water Crisis Hits Rich Countries, World Wildlife Fund, 2006

Wilhite, D.A., 2000. Drought as a natural hazard: concepts and definitions.

World Meteorological Organization (WMO), 2005. Drought Assessment and Forecasting. Available at: <http://www.wmo.int/pages/prog/hwrp/documents/regions/DOC8.pdf>

World Population Prospects (2017 Revision) - United Nations population estimates and projections.

Zhai, J., Su, B., Krysanova, V., Vetter, T., Gao, C. and Jiang, T., 2010. Spatial variation and trends in PDSI and SPI indices and their relation to streamflow in 10 large regions of China. *Journal of Climate*, 23(3), pp.649-663.

Zhai, J.Q., Liu, B., Hartmann, H., Da Su, B., Jiang, T. and Fraedrich, K., 2010. Dryness/wetness variations in ten large river basins of China during the first 50 years of the 21st century. *Quaternary International*, 226(1-2), pp.101-111.

Zhang, X., Tang, Q., Liu, X., Leng, G. and Li, Z., 2017. Soil moisture drought monitoring and forecasting using satellite and climate model data over southwestern China. *Journal of Hydrometeorology*, 18(1), pp.5-23.

Ziv, G., Baran, E., Nam, S., Rodríguez-Iturbe, I. and Levin, S.A., 2012. Trading-off fish biodiversity, food security, and hydropower in the Mekong River Basin. *Proceedings of the National Academy of Sciences*, p.201201423.